Inorganic Chemistry

Article

pubs.acs.org/IC

Synthesis, Reactivity Studies, Structural Aspects, and Solution Behavior of Half Sandwich Ruthenium(II) *N,N′,N″*-Triarylguanidinate Complexes

Taruna Singh,[†] Ram Kishan,[†] Munirathinam Nethaji,[‡] and Natesan Thirupathi*[,†]

[†]Department of Chemistry, University of Delhi, Delhi 110 007, India

[‡]Department of Inorganic and Physical Chemistry, Indian Institute of Science, Bangalore 560 012, India

Supporting Information

ABSTRACT: $[(\eta^6\text{-}C_{10}H_{14})RuCl(\mu\text{-}Cl)]_2$ ($\eta^6\text{-}C_{10}H_{14}$ = η^6-*p*-cymene) was subjected to a bridge-splitting reaction with *N,N′,N″*-triarylguanidines, $(ArNH)_2C{=}NAr$, in toluene at ambient temperature to afford $[(\eta^6\text{-}C_{10}H_{14})RuCl\{\kappa^2(N,N')((ArN)_2C{-}N(H)Ar)\}]$ (Ar = $C_6H_4Me{-}4$ (**1**), $C_6H_4(OMe){-}2$ (**2**), $C_6H_4Me{-}2$ (**3**), and $C_6H_3Me_2{-}2,4$ (**4**)) in high yield with a view aimed at understanding the influence of substituent(s) on the aryl rings of the guanidine upon the solid-state structure, solution behavior, and reactivity pattern of the products. Complexes **1**−**3** upon reaction with NaN_3 in ethanol at ambient temperature afforded $[(\eta^6\text{-}C_{10}H_{14})RuN_3\{\kappa^2(N,N')((ArN)_2C{-}N(H)Ar)\}]$ (Ar = $C_6H_4Me{-}4$ (**5**), $C_6H_4(OMe){-}2$ (**6**), and $C_6H_4Me{-}2$ (**7**)) in high yield. [3 + 2] cycloaddition reaction of **5**−**7** with RO(O)C−C≡C−C(O)OR (R = Et (DEAD) and Me (DMAD)) (diethylacetylenedicarboxylate, DEAD; dimethylacetylenedicarboxylate, DMAD) in CH_2Cl_2 at ambient temperature afforded $[(\eta^6\text{-}C_{10}H_{14})Ru\{N_3C_2(C(O)OR)_2\}\{\kappa^2(N,N')((ArN)_2C{-}N(H)Ar)\}]\cdot xH_2O$ (x = 1, R = Et, Ar = $C_6H_4Me{-}4$ (**8**·H_2O); x = 0, R = Me, Ar = $C_6H_4(OMe){-}2$ (**9**), and $C_6H_4Me{-}2$ (**10**)) in moderate yield. The molecular structures of **1**−**6**, **8**·H_2O, and **10** were determined by single crystal X-ray diffraction data. The ruthenium atom in the aforementioned complexes revealed pseudo octahedral "three legged piano stool" geometry. The guanidinate ligand in **2**, **3**, and **6** revealed *syn-syn* conformation and that in **4**, and **10** revealed *syn-anti* conformation, and the conformational difference was rationalized on the basis of subtle differences in the stereochemistry of the coordinated nitrogen atoms caused by the aryl moiety in **3** and **4** or steric overload caused by the substituents around the ruthenium atom in **10**. The bonding pattern of the CN_3 unit of the guanidinate ligand in the new complexes was explained by invoking n−π conjugation involving the interaction of the $NHAr/N_{coord}Ar$ lone pair with C=Nπ^* orbital of the imine unit. Complexes **1**, **2**, **5**, **6**, **8**·H_2O, and **9** were shown to exist as a single isomer in solution as revealed by NMR data, and this was ascribed to a fast C−N(H)Ar bond rotation caused by a less bulky aryl moiety in these complexes. In contrast, **3** and **10** were shown to exist as a mixture of three and five isomers in about 1:1:1 and 1·0:1·2:2·7:3·5:6·9 ratios, respectively in solution as revealed by a VT ^1H NMR, $^1H{-}^1H$ COSY in conjunction with DEPT−90 ^{13}C NMR data measured at 233 K in the case of **3**. The multiple number of isomers in solution was ascribed to the restricted C−N(H)(*o*-tolyl) bond rotation caused by the bulky *o*-tolyl substituent in **3** or the aforementioned restricted C−NH(*o*-tolyl) bond rotation as well as the restricted ruthenium-arene(centroid) bond rotation caused by the substituents around the ruthenium atom in **10**.

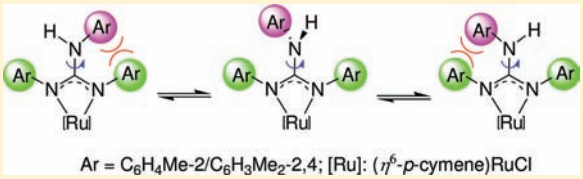

INTRODUCTION

Half sandwich ruthenium(II) amido complexes play a vital role as enantioselective catalysts in numerous organic transformations,[1] as anticancer agents,[2] as protein and lipid kinase inhibitors,[3] and as a potential organometallic molecular motors.[4] Further, this class of complexes are shown to be a useful promoter for peptide synthesis,[5] as scaffolds to study the intriguing structural, reactivity pattern and bonding aspects.[6−16] *N,N′,N″*-Trisubstituted guanidines, $(RNH)_2C{=}NR$ (R = alkyl, aryl and acetyl) is one of the interesting classes of *N*-donor ligands because of their ability to form guanidinate(1−) (**A**) and guanidinate(2−) (**B**) anions upon treatment with a strong base (Chart 1). Further, the donor characteristics, steric environment around the nitrogen atoms of this type of guanidines may be finely controlled by introducing distinct substituents on the nitrogen atoms.

The coordination chemistry aspects of $(RNH)_2C{=}NR$ (R = Ph (LH_2^{Ph}), *i*Pr (LH_2^{iPr}), and Cy (LH_2^{Cy})) have been explored recently and these ligands have been shown to exhibit a rich and diverse coordination modes toward metal ions depending upon the substituent on the nitrogen atoms.[17−19] Several structurally characterized ruthenium(II) guanidinate(1−) complexes of LH_2^{Ph} and one ruthenium(II) guanidinate(2−) complex of $(AcNH)_2C{=}NAc$ (Ac = C(O)Me; LH_2^{Ac}) are known wherein the guanidinate ligand is shown to exhibit

Received: June 22, 2011
Published: December 8, 2011

Chart 1. Structures of Guanidinate(1−) and Guanidinate(2−) Anions

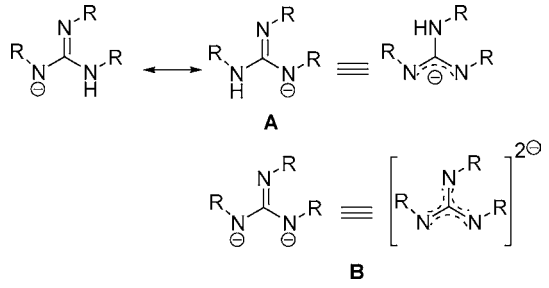

chelating bidentate, and bridging bidentate coordination modes.[20,21] The molecular structures of half-sandwich ruthenium(II) guanidinate(1−) complexes, $[(\eta^6\text{-}C_{10}H_{14})RuCl\{\kappa^2(N,N')((RN)_2C{-}N(H)R)\}]$ (R = Ph (**I**),[22] and *i*Pr (**II**)[23]) have also been determined but the results pertinent to **II** remain unpublished.

In 2010, we have published synthesis and conformational features of *sym N,N′,N″*-triarylguanidines, $(ArNH)_2C{=}NAr$ (Ar = $C_6H_4Me{-}4$ ($LH_2^{4\text{-tolyl}}$), $C_6H_4Me{-}2$ ($LH_2^{2\text{-tolyl}}$), $C_6H_4(OMe){-}2$ ($LH_2^{2\text{-anisyl}}$), $C_6H_3Me_2{-}3,5$ ($LH_2^{3,5\text{-xylyl}}$), $C_6H_3Me_2{-}2,4$ ($LH_2^{2,4\text{-xylyl}}$), and $C_6H_3Me_2{-}2,6$ ($LH_2^{2,6\text{-xylyl}}$)),[24] and subsequently we have reported the synthesis, reactivity studies, structural aspects, and solution dynamics of $LH_2^{2\text{-anisyl}}$ derived six-membered [*C,N*] palladacycles.[25] Herein, we report the synthesis and characterization of three types of half-sandwich ruthenium(II) guanidinate complexes, namely $[(\eta^6\text{-}C_{10}H_{14})RuX\{\kappa^2(N,N')((ArN)_2C{-}N(H)Ar)\}]$ (X = Cl; Ar = $C_6H_4Me{-}4$ (**1**), $C_6H_4(OMe){-}2$ (**2**), $C_6H_4Me{-}2$ (**3**), $C_6H_3Me_2{-}2,4$ (**4**) and X = N_3; Ar = $C_6H_4Me{-}4$ (**5**), $C_6H_4(OMe){-}2$ (**6**), and $C_6H_4Me{-}2$ (**7**)), and the triazole derivatives, $[(\eta^6\text{-}C_{10}H_{14})Ru\{N_3C_2(C(O)OR)_2\}\text{-}\{\kappa^2(N,N')((ArN)_2C{-}N(H)Ar)\}]\cdot xH_2O$ (x = 1, R = Et, Ar = $C_6H_4Me{-}4$ (**8**·H_2O); x = 0, R = Me, Ar = $C_6H_4(OMe){-}2$ (**9**), and $C_6H_4Me{-}2$ (**10**)). Complex **3** revealed a unique fluxional behavior in that it exists as a mixture of three rotamers in solution at temperatures ≤253 K and equilibrate via a restricted C−N(H)(*o*-tolyl) bond rotation caused by the bulky *o*-tolyl substituent of the guanidinate ligand.

EXPERIMENTAL SECTION

General Procedures. *N,N′,N″*-Triarylguanidines ($LH_2^{4\text{-tolyl}}$, $LH_2^{2\text{-tolyl}}$, $LH_2^{2\text{-anisyl}}$, $LH_2^{2,4\text{-xylyl}}$, and $LH_2^{2,6\text{-xylyl}}$)),[24] and $[(\eta^6\text{-}C_{10}H_{14})\text{-}RuCl(\mu\text{-}Cl)]_2$[26] were prepared following the literature procedures. $RuCl_3\cdot xH_2O$, RO(O)C−C≡C−C(O)OR (R = Me (DMAD), and Et (DEAD)), NaN_3, and deuterated solvents were purchased from Sigma-Aldrich and used as received. The IR spectral data were obtained using KBr pellets on Shimadzu IR435 spectrometer in the frequency range 400−4000 cm^{-1}. TOF−MS spectra were recorded on a Micromass LCT KC 455 instrument using electrospray positive ion mode. ^1H and ^{13}C NMR spectra were recorded on an Avance Bruker−300 NMR spectrometer operating at 300 and 75.5 MHz, respectively and JEOL ECX 400 NMR spectrometer operating at 400 and 100 MHz, respectively. The chemical shifts are reported in parts per million (ppm) relative to tetramethylsilane or residual solvent signal. A variable temperature (VT) ^1H NMR spectra of **2**, **3**, and **10**, and DEPT−90 ^{13}C NMR spectrum of **3** were recorded on Bruker AV−400 NMR spectrometer operating at 400, and 100 MHz, respectively. Melting points of **1**−**3** were recorded on Buchi melting point apparatus (Model: M−560), and the reported values are uncorrected. The TGA/DTA thermogram of **8**·H_2O was measured on PerkinElmer Diamond instrument under nitrogen atmosphere at 2 °C/min heating rate.

Caution! *Metal azido complexes are potentially explosive, only a small amount of material should be prepared with care.*

Synthesis, Analytical and Spectroscopic Data of 1−10. *$[(\eta^6\text{-}C_{10}H_{14})RuCl\{\kappa^2(N,N')((ArN)_2C{-}N(H)Ar)\}]$ (Ar = $C_6H_4Me{-}4$; **1**).* $[(\eta^6\text{-}C_{10}H_{14})RuCl(\mu\text{-}Cl)]_2$ (100 mg, 0.163 mmol) was dispersed in toluene (10 mL) in a 25 mL round-bottom flask and set to stir. To the suspension, $LH_2^{4\text{-tolyl}}$ (215 mg, 0.653 mmol) was added in a portion that immediately resulted in the formation of $[LH_3^{4\text{-tolyl}}]^+Cl^-$ as colorless solid. The reaction mixture was stirred for 2 h at ambient temperature and filtered. The filtrate was concentrated under vacuum to about 2 mL, and the concentrate was stored at ambient temperature for several hours to afford **1** as orange crystals. Yield: 90% (175 mg, 0.292 mmol). Mp: 132 °C (decomp). IR (KBr, cm^{-1}) ν_{max}: 3372 (m, NH), 1543 (vs, C=N). ^1H NMR (400 MHz, $CDCl_3$, ppm): δ_H = 1.22 (d, $J_{H,H}$ = 6.8 Hz, 6H, $CH(CH_3)_2$), 2.09 (s, 3H, CH_3), 2.21 (s, 2 × 3H, CH_3), 2.22 (s, 3H, CH_3), 2.68−2.75 (m, 1H, $CHMe_2$), 5.08, 5.32 (each d, $J_{H,H}$ = 6.0 Hz, 4H, C_6H_4), 5.88 (s, 1H, N*H*), 6.64, 6.70 (each d, $J_{H,H}$ = 8.2 Hz, 4H, Ar*H*), 6.91 (d, $J_{H,H}$ = 8.3 Hz, 4H, Ar*H*), 7.05 (d, $J_{H,H}$ = 8.2 Hz, 4H, Ar*H*). $^{13}C\{^1H\}$ NMR (100 MHz, $CDCl_3$, ppm): δ_C = 19.1 (CH_3), 20.6, 20.9 (CH_3), 22.5 ($CH(CH_3)_2$), 31.3 ($CHMe_2$), 78.7, 80.8, 97.8, 98.4 (*p*-cymene Ar*C*), 119.9, 123.3, 128.9, 129.2, 129.8, 131.5, 131.7, 135.5, 144.3, 154.0 (Ar*C* and C=N). Note: Only two carbon resonances were observed for CH_3 carbon of the guanidinate ligand rather than the expected three peaks and 10 carbon resonances were observed for Ar*C* and *C*=N carbons of the guanidinate ligand rather than the expected 13 peaks, presumably because of overlapping peaks. TOF−MS^+, *m/z* [ion, intensity (%)]: 601.097 [$(M + 2H)^+$, 60], 599.088 [M^+, 28], 328.316 [$(LH_2^{4\text{-tolyl}} - H)^+$, 100]. Anal. Calcd. for $C_{32}H_{36}N_3ClRu$ (M_w: 599.17): C, 64.15; H, 6.06; N, 7.01. Found: C, 64.14; H, 6.06; N, 7.01.

*$[(\eta^6\text{-}C_{10}H_{14})RuCl\{\kappa^2(N,N')((ArN)_2C{-}N(H)Ar)\}]$ (Ar = $C_6H_4(OMe){-}2$; **2**).* Complex **2** was prepared from $[(\eta^6\text{-}C_{10}H_{14})RuCl(\mu\text{-}Cl)]_2$ (100 mg, 0.163 mmol) and $LH_2^{2\text{-anisyl}}$ (258 mg, 0.684 mmol) in toluene (10 mL) following the procedure previously described for **1**. The filtrate from the reaction mixture was concentrated under vacuum to about 2 mL and stored at ambient temperature for several hours to afford **2** as orange crystals. Yield: 95% (200 mg, 0.309 mmol). Mp: 116 °C (decomp). IR (KBr, cm^{-1}) ν_{max}: 3419 (br, NH), 3330 (m, NH), 2929 (m, C−H···Cl), 1534 (vs, C=N). ^1H NMR (400 MHz, CD_2Cl_2, ppm): δ_H = 1.19 (d, $J_{H,H}$ = 6.8 Hz, 6H, $CH(CH_3)_2$), 2.19 (s, 3H, CH_3), 2.57−2.64 (m, 1H, $CHMe_2$), 3.76 (s, 3H, OCH_3), 3.80 (s, 2 × 3H, OCH_3), 5.07, 5.24 (each d, $J_{H,H}$ = 6.0 Hz, 4H, C_6H_4), 6.25 (dt, $J_{H,H}$ = 7.6; 1.2 Hz, 1H, Ar*H*), 6.52 (dt, $J_{H,H}$ = 8.3; 1.6 Hz, 1H, Ar*H*), 6.59 (dt, $J_{H,H}$ = 7.6; 1.5 Hz, 2H, Ar*H*), 6.68 (dd, $J_{H,H}$ = 7.8; 1.8 Hz, 2H, Ar*H*), 6.83 (dt, $J_{H,H}$ = 7.4; 1.6 Hz, 2H, Ar*H*), 6.88 (dt, $J_{H,H}$ = 7.5; 1.9 Hz, 2H, Ar*H*), 7.30 (s, 1H, N*H*), 7.39 (dd, $J_{H,H}$ = 7.6; 2.0 Hz, 2H, Ar*H*). $^{13}C\{^1H\}$ NMR (75.5 MHz, $CDCl_3$, ppm): δ_C = 18.7 (CH_3), 22.1 ($CH(CH_3)_2$), 30.9 ($CHMe_2$), 55.1, 55.3, 55.7 (OCH_3), 79.6, 79.8, 96.1, 99.1 (*p*-cymene Ar*C*), 108.7, 110.5, 111.0, 119.6, 120.5, 120.6, 121.0, 122.7, 124.0 (br), 125.1, 126.4 (br), 127.0, 136.8, 147.2, 151.3, 152.0, 153.8 (Ar*C* and *C*=N). Note: Only 17 carbon resonances were observed for Ar*C* and *C*=N carbons of the guanidinate ligand rather than the expected 19 peaks, presumably because of overlapping peaks. Three rotamers were observed in about 1.0:0.05:0.04 ratios in CD_3CN as estimated from the integrals of *p*-cymene C*H* protons. ^1H NMR (400 MHz, CD_3CN, ppm): δ_H = 1.16 (d, $J_{H,H}$ = 6.9 Hz, $CH(CH_3)_2$, rotamers 1, 2 or 3), 1.30 (d, $J_{H,H}$ = 6.4 Hz, $CH(CH_3)_2$, rotamer 2 or 3), 2.10−2.33 (br, CH_3, rotamers 1, 2 and 3), 2.48−2.55 (m, $CHMe_2$, rotamers 1, 2 or 3), 2.89−2.93 (m, $CHMe_2$, rotamer 2 or 3), 3.77, 3.79, 3.83, 3.88 (s, OCH_3, rotamers 1, 2 and 3), 5.10, 5.24 (each d, $J_{H,H}$ = 5.3 Hz, C_6H_4, rotamer 1), 5.28, 5.43, 5.54 (each br, C_6H_4, rotamers 2 and 3), 6.19 (apparent t, $J_{H,H}$ = 7.1 Hz, Ar*H*), 6.53 (m, Ar*H*), 6.64 (d, $J_{H,H}$ = 7.8 Hz, Ar*H*), 6.73 (d, $J_{H,H}$ = 6.9 Hz, Ar*H*), 6.84−6.92 (m, Ar*H*), 7.06−7.09 (m, Ar*H*), 7.28 (d, $J_{H,H}$ = 7.3 Hz, Ar*H*), 7.37 (d, $J_{H,H}$ = 6.4 Hz, Ar*H*), 7.49 (Ar*H*), 8.61(br, N*H*). $^{13}C\{^1H\}$ NMR (100 MHz, CD_3CN, ppm): δ_C = 19.0 (CH_3), 22.4 ($CH(CH_3)_2$), 31.9 ($CHMe_2$), 56.0, 56.1, 56.4 (OCH_3), 80.6, 80.8, 97.0, 99.9 (*p*-cymene Ar*C*), 110.3, 111.8, 112.4, 119.8, 120.1, 121.5, 121.6, 123.8, 125.3, 125.8, 127.2, 127.8, 128.4, 137.6, 148.3, 151.3, 153.0, 153.1, 154.4 (Ar*C* and *C*=N). The NMR peak assignments reported in CD_3CN were independently

dx.doi.org/10.1021/ic201343w | *Inorg. Chem.* 2012, 51, 157−169

confirmed by two-dimensional HETCOR NMR data (Figures S1−S3 in the Supporting Information). TOF−MS$^+$, m/z [ion, intensity (%)]: 648.5574 [(M + H)$^+$, 8]. Anal. Calcd. for $C_{32}H_{36}N_3ClO_3Ru$ (M_w: 647.17): C, 59.39; H, 5.60; N, 6.49. Found: C, 59.62; H, 5.75; N, 6.75.

*[(η^6-$C_{10}H_{14}$)RuCl{κ^2(N,N′)((ArN)$_2$C−N(H)Ar)}] (Ar = C_6H_4Me−2; **3**).* Complex **3** was prepared from [(η^6-$C_{10}H_{14}$)RuCl(μ-Cl)]$_2$ (100 mg, 0.163 mmol) and $LH_2^{2\text{-tolyl}}$ (225 mg, 0.683 mmol) in toluene (10 mL) following the procedure previously described for **1**. The filtrate from the reaction mixture was concentrated under vacuum to about 2 mL and stored at ambient temperature for several hours to afford **3** as orange crystals. Yield: 92% (180 mg, 0.300 mmol). Mp: 120 °C(decomp). IR (KBr, cm^{-1}) ν_{max}: 3435 (br, NH), 2924 (vs, C−H···Cl), 2853 (s, C−H···Cl), 1591 (s, C═N). ^{1}H NMR (300 MHz, $CDCl_3$, ppm): δ_H = 1.17 (br, CH(CH_3)$_2$), 1.95, 2.00, 2.12, 2.22, 2.37 (br, CH_3), 2.58 (br, CH_3/CH), 5.05, 5.32 (each br, C_6H_4), 6.69−7.23 (br m), 7.49 (br, ArH and NH). Complex **3** revealed broad featureless ^{13}C NMR signals presumably because of its fluxional behavior and thus precluded the unambiguous assignment of ^{13}C NMR data. TOF−MS$^+$, m/z [ion, intensity (%)]: 599.5474 [M$^+$, 5], 327.4343 [($LH_2^{2\text{-tolyl}}$ − 2H)$^+$, 97]. Anal. Calcd for $C_{32}H_{36}N_3ClRu$ (M_w: 599.17): C, 64.15; H, 6.06; N, 7.01. Found: C, 64.33; H, 6.14; N, 6.78.

*[(η^6-$C_{10}H_{14}$)RuCl{κ^2(N,N′)((ArN)$_2$C−N(H)Ar)}] (Ar = $C_6H_3Me_2$−2,4; **4**).* [(η^6-$C_{10}H_{14}$)RuCl(μ-Cl)]$_2$ (100 mg, 0.163 mmol) was dispersed in toluene (10 mL) in a 25 mL round-bottom flask. To the suspension, $LH_2^{2,4\text{-xylyl}}$ (255 mg, 0.686 mmol) was added in a portion that immediately resulted in the formation of [$LH_3^{2,4\text{-xylyl}}$]$^+$Cl$^-$ as colorless solid. The reaction mixture was stirred for 2 h at room temperature and filtered. The volatiles from the filtrate were removed under vacuum to afford a gummy solid. The gummy solid was extracted with diisopropyl ether, and the extract was left at ambient temperature for 24 h to afford **4** as orange crystals. Yield: 79% (165 mg, 0.257 mmol). IR (KBr, cm^{-1}) ν_{max}: 3386 (w, NH), 2962 (s, C−H···Cl), 2921 (s, C−H···Cl), 1543 (m, C═N). The ^{1}H NMR spectrum of **4** revealed the presence of three isomers in about 1.0:1.1:3.8 ratios as estimated from the integrals of CH(CH_3)$_2$ protons. ^{1}H NMR (300 MHz, $CDCl_3$, ppm): δ_H = 1.09 (d, $J_{H,H}$ = 6.3 Hz, CH(CH_3)$_2$, major isomer), 1.14 (d, $J_{H,H}$ = 6.9 Hz, CH(CH_3)$_2$, minor isomer 1), 1.21 (d, $J_{H,H}$ = 6.9 Hz, CH(CH_3)$_2$, minor isomer 2), 1.86, 1.92, 1.95 (each s, CH_3), 2.11 (br, CH_3), 2.29 (br, CH_3), 2.55−2.65 (m, $CHMe_2$, major and minor isomers), 4.91−5.10 (br, C_6H_4), 5.20−5.28 (br, C_6H_4), 5.41 (d, $J_{H,H}$ = 6.0 Hz, C_6H_4), 6.40−7.10 (br), 7.30 (br, ArH and NH). TOF−MS$^+$, m/z [ion, intensity (%)]: 641.6260 [M$^+$, 37]. Anal. Calcd for $C_{35}H_{42}N_3ClRu$ (M_w: 641.26): C, 65.56; H, 6.60; N, 6.55. Found: C, 65.09; H, 6.44; N, 6.67. Multiple attempts to obtain a better carbon value were unsuccessful.

The reaction of [(η^6-$C_{10}H_{14}$)RuCl(μ-Cl)]$_2$ (100 mg, 0.163 mmol) with $LH_2^{2,6\text{-xylyl}}$ (255 mg, 0.686 mmol) in toluene (10 mL) at ambient temperature did not afford any product as verified by TLC.

*[(η^6-$C_{10}H_{14}$)RuN$_3${κ^2(N,N′)((ArN)$_2$C−N(H)Ar)}] (Ar = C_6H_4Me−4; **5**).* To a solution of **1** (100 mg, 0.167 mmol) in ethanol (10 mL) was added NaN_3 (22.0 mg, 0.338 mmol), and the resulting homogeneous solution was stirred at ambient temperature for 6 h. The reaction mixture was concentrated under vacuum to afford a residue. The product was extracted from the residue with diethyl ether (20 mL) and filtered. The filtrate was concentrated under vacuum to about 5 mL and stored at −10 °C for 24 h to afford **5** as red crystals. Yield: 82% (83 mg, 0.137 mmol). IR (KBr, cm^{-1}) ν_{max}: 3398 (w, NH), 2030 (vs, N_3), 1543 (s, C═N). ^{1}H NMR (400 MHz, $CDCl_3$, ppm): δ_H = 1.22 (d, $J_{H,H}$ = 6.8 Hz, 6H, CH(CH_3)$_2$), 2.09 (s, 3H, CH_3), 2.21 (s, 2 × 3H, CH_3), 2.22 (s, 3H, CH_3), 2.68−2.75 (m, 1H, $CHMe_2$), 5.08, 5.33 (each d, $J_{H,H}$ = 6.0 Hz, 4H, C_6H_4), 5.88 (s, 1H, NH), 6.64 (d, $J_{H,H}$ = 8.7 Hz, 2H, ArH), 6.70 (d, $J_{H,H}$ = 8.2 Hz, 2H, ArH), 6.90 (d, $J_{H,H}$ = 8.3 Hz, 4H, ArH), 7.05 (d, $J_{H,H}$ = 8.2 Hz, 4H, ArH). ^{13}C{^{1}H} NMR (100 MHz, $CDCl_3$, ppm): δ_C = 19.2 (CH_3), 20.7, 21.0 (CH_3), 22.6 (CH(CH_3)$_2$), 31.5 (CH(CH_3)$_2$), 78.8, 80.9, 97.9, 98.5 (*p*-cymene ArC), 120.0, 123.4, 129.0, 129.3, 130.0, 131.6, 131.9, 135.6, 144.3, 154.1 (ArC and C═N). Note: Only 2 carbon resonances were observed for CH_3 carbon rather than the expected 3 peaks, and 10 carbon resonances were observed for ArC and C═N carbons of the guanidinate ligand rather than the expected 13 peaks, presumably because of overlapping peaks. Anal. Calcd for $C_{32}H_{36}N_6Ru{\cdot}H_2O$ (M_w: 623.76): C, 61.62; H, 6.14; N, 13.47. Found: C, 62.03; H, 6.00; N, 13.80.

*[(η^6-$C_{10}H_{14}$)RuN$_3${κ^2(N,N′)((ArN)$_2$C−N(H)Ar)}] (Ar = C_6H_4(OMe)−2; **6**).* Complex **6** was prepared from **2** (100 mg, 0.154 mmol) and NaN_3 (20.0 mg, 0.308 mmol) in ethanol (10 mL) following the procedure previously described for **5**. The sample was crystallized from diethyl ether at −10 °C over a period of 24 h. Yield: 82% (83 mg, 0.127 mmol). IR (KBr, cm^{-1}) ν_{max}: 3336 (w, NH), 2026 (s, N_3), 1531 (s, C═N). ^{1}H NMR (300 MHz, $CDCl_3$, ppm): δ_H = 1.20 (d, $J_{H,H}$ = 6.9 Hz, 6H, CH(CH_3)$_2$), 2.14 (s, 3H, CH_3), 2.55−2.59 (m, 1H, $CHMe_2$), 3.75 (s, 3H, OCH_3), 3.85 (s, 2 × 3 H, OCH_3), 4.94, 5.08 (each d, $J_{H,H}$ = 4.5 Hz, 4H, C_6H_4), 6.33 (br m, 1H, ArH), 6.54 (br, 2H, ArH), 6.69, 6.72 (each s, 2H, ArH), 6.78−6.90 (m, 5H, ArH), 7.28 (s, 2H, ArH), 7.39 (s, 1H, NH). ^{13}C{^{1}H} NMR (100 MHz, $CDCl_3$, ppm): δ_C = 18.22 (CH_3), 22.50 (CH(CH_3)$_2$), 30.91 ($CHMe_2$), 55.34, 55.47 (OCH_3), 79.71, 80.12, 95.78, 100.22 (*p*-cymene ArC), 108.94, 110.77, 120.06, 120.59, 120.64, 120.92, 121.30, 123.23, 124.96, 127.14, 127.23, 137.09, 147.42, 147.45, 152.17, 154.88, 154.91 (ArC and C═N). Note: Only two carbon resonances were observed for OCH_3 carbon rather than the expected 3 peaks and 17 carbon resonances were observed for ArC and C═N carbons of the guanidinate ligand rather than the expected 19 peaks, presumably because of overlapping peaks. Anal. Calcd for $C_{32}H_{36}N_6O_3Ru$ (M_w: 653.74): C, 58.79; H, 5.55; N, 12.86. Found: C, 58.94; H, 5.64; N, 12.56.

*[(η^6-$C_{10}H_{14}$)RuN$_3${κ^2(N,N′)((ArN)$_2$C−N(H)Ar)}] (Ar = C_6H_4Me−2; **7**).* Complex **7** was prepared from **3** (100 mg, 0.167 mmol) and NaN_3 (22.0 mg, 0.338 mmol) in ethanol (10 mL) following the procedure previously described for **5**. Complex **7** was crystallized from diethyl ether at −10 °C over a period of several hours. Yield: 94% (94 mg, 0.155 mmol). IR (KBr, cm^{-1}) ν_{max}: 3295 (br w, NH), 2028 (vs, N_3), 1541 (s, C═N). The ^{1}H NMR spectrum of **7** revealed the presence of two isomers as inferred from CH_3 signals of the *i*Pr moiety, but their relative ratio was difficult to estimate because of overlapping peaks. ^{1}H NMR (300 MHz, $CDCl_3$, ppm): δ_H = 1.10−1.20 (br, CH(CH_3)$_2$, major isomer), 1.24 (d, $J_{H,H}$ = 8.4 Hz, CH(CH_3)$_2$, minor isomer), 1.87 (CH_3), 2.03 (br, CH_3), 2.09 (CH_3), 2.40 (CH_3), 2.45 (br, CH_3), 2.62−2.66 (m, $CHMe_2$), 3.47−3.49 (m, $CHMe_2$), 4.91, 5.08, 5.25, 5.27, 5.32, 5.34 (each br, C_6H_4), 6.60−7.15 (br m, ArH and NH). Anal. Calcd for $C_{32}H_{36}N_6Ru$ (M_w: 605.74): C, 63.45; H, 5.99; N, 13.87. Found: C, 63.71; H, 6.04; N, 13.52.

*[(η^6-$C_{10}H_{14}$)Ru{N_3C_2(C(O)OEt)$_2$}{κ^2(N,N′)((ArN)$_2$C−N(H)Ar)}]·H_2O (Ar = C_6H_4Me−4; **8**·H_2O).* Complex **5** (100 mg, 0.165 mmol) was dissolved in CH_2Cl_2 (5 mL) in a 25 mL round-bottom flask. To the aforementioned solution, a CH_2Cl_2 (5 mL) solution of DEAD (56 mg, 0.330 mmol) was slowly added, stirred at room temperature for 24 h, and concentrated under vacuum to about 2 mL. The concentrate was layered with *n*-hexane (5 mL) and stored at ambient temperature for 24 h to afford **8**·H_2O as yellow crystals. Yield: 60% (78 mg, 0.098 mmol). IR (KBr, cm^{-1}) ν_{max}: 3326 (m, NH), 1725, 1710 (each s, C═O), 1540 (s, C═N), 1439 (s, N═N), 1290 (m, C−O). ^{1}H NMR (400 MHz, $CDCl_3$, ppm): δ_H = 1.16 (d, $J_{H,H}$ = 7.0 Hz, 6H, CH(CH_3)$_2$), 1.29 (t, $J_{H,H}$ = 7.2 Hz, 6H, CH_2CH_3), 2.01 (s, 3H, CH_3), 2.08 (s, 3H, CH_3), 2.19 (s, 2 × 3H, CH_3), 2.67−2.72 (m, 1H, $CHMe_2$), 4.28 (q, $J_{H,H}$ = 7.2 Hz, 4H, CH_2CH_3), 5.27, 5.45 (each d, $J_{H,H}$ = 5.9 Hz, 4H, C_6H_4), 5.85 (s, 1H, NH), 6.62 (d, $J_{H,H}$ = 8.4 Hz, 2H, ArH), 6.68 (d, $J_{H,H}$ = 8.4 Hz, 2H, ArH), 6.85 (d, $J_{H,H}$ = 8.4 Hz, 4H, ArH), 6.89 (d, $J_{H,H}$ = 8.4 Hz, 4H, ArH). ^{13}C{^{1}H} NMR (100 MHz, $CDCl_3$, ppm): δ_C = 14.3 (CH_2CH_3), 18.7 (CH_3), 20.7, 20.9 (CH_3), 22.7 (CH(CH_3)$_2$), 31.2 ($CHMe_2$), 60.6 (CH_2CH_3), 81.1, 83.0, 98.8, 101.2 (*p*-cymene ArC), 120.0, 123.5, 128.8, 129.2, 131.6, 131.7, 135.6, 139.8, 144.4, 155.3 (ArC and C═N), 163.0 (OC(O)). Only 5 carbon signals were observed for CH_3 carbon rather than the expected 6 peaks, and 10 carbon resonances were observed for ArC and C═N carbons of the guanidinate and the triazolate ligands rather than the expected 14 peaks, presumably because of overlapping peaks. Anal. Calcd for $C_{40}H_{46}N_6O_4Ru{\cdot}H_2O$ (M_w: 793.93): C, 60.51; H, 6.09; N, 10.58. Found: C, 60.23; H, 5.76; N, 10.83.

dx.doi.org/10.1021/ic201343w | *Inorg. Chem.* 2012, 51, 157−169

Table 1. Crystallographic Data for 1−4

	1	2	3	4
formula	$C_{32}H_{36}N_3ClRu$	$C_{32}H_{36}N_3ClO_3Ru$	$C_{32}H_{36}N_3ClRu$	$C_{35}H_{42}N_3ClRu$
Fw	599.16	647.16	599.16	641.24
T/K	298(2)	100(2)	100(2)	100(2)
λ/Å	0.71073	0.71073	0.71073	0.71073
cryst syst	monoclinic	monoclinic	monoclinic	monoclinic
space group	$P2_1/n$	$P2_1$	$P2_1$	$C2/c$
a/Å	15.844(5)	18.565(2)	10.355(5)	14.4275(13)
b/Å	9.534(5)	8.3952(11)	8.834(5)	14.3557(13)
c/Å	19.696(5)	19.908(2)	15.100(5)	30.288(3)
α/deg	90	90	90	90
β/deg	103.756(5)	109.837(5)	94.342(5)	90.809(7)
γ/deg	90	90	90	90
V/Å^3	2889.9(19)	2918.8(6)	1377.3(11)	6272.6(10)
Z	4	4	2	8
D_{calcd}/g cm^{-3}	1.377	1.473	1.445	1.358
$F(000)$	1240	1336	620	2672
μ/mm^{-1}	0.660	0.667	0.692	0.613
θ range/deg	3.0−26.4	1.09−28.32	1.35−27.92	1.34−28.45
reflns measured	5890	14327	6275	7812
reflns used	4649	13184	5551	5892
parameters	340	734	340	371
$R1$	0.0403	0.0327	0.0378	0.0532
$wR2$	0.1079	0.0704	0.1032	0.1345
goodness of fit on F^2	1.051	1.180	1.203	1.124

Table 2. Crystallographic Data for 5, 6, 8·H_2O, and 10

	5	6	8·H_2O	10
formula	$C_{32}H_{36}N_6Ru$	$C_{32}H_{36}N_6O_3Ru$	$C_{80}H_{92}N_{12}O_9Ru_2$	$C_{38}H_{42}N_6O_4Ru$
Fw	605.74	653.74	1567.80	747.85
T/K	298(2)	298(2)	298(2)	298(2)
λ/Å	0.71073	0.71073	0.71073	0.71073
cryst syst	orthorhombic	orthorhombic	monoclinic	triclinic
space group	$P2_12_12_1$	$P2_12_12_1$	$C2/c$	$P\bar{1}$
a/Å	8.3950(2)	9.1199(2)	32.390(5)	10.277(5)
b/Å	13.1183(3)	17.6750(6)	13.2154(9)	11.060(5)
c/Å	26.1858(8)	18.9166(5)	25.888(4)	16.638(5)
α/deg	90	90	90	70.932(5)
β/deg	90	90	136.05(3)	77.569(5)
γ/deg	90	90	90	82.911(5)
V/Å^3	2883.79(13)	3049.24(15)	7691(5)	1742.6(13)
Z	4	4	4	2
D_{calcd}/g cm^{-3}	1.395	1.424	1.354	1.425
$F(000)$	1256	1352	3264	776
μ/mm^{-1}	0.575	0.557	0.457	0.499
θ range/deg	2.98−26.37	3.10−26.37	3.08−26.37	1.32−23.35
reflns measured	5665	5684	7849	4832
reflns used	4787	4697	6582	4010
parameters	358	385	473	453
$R1$	0.0357	0.0331	0.0394	0.0503
$wR2$	0.0803	0.0532	0.0918	0.1391
goodness of fit on F^2	0.974	0.865	1.031	1.142

*[(η^6-$C_{10}H_{14}$)Ru{N_3C_2(C(O)OMe)$_2$}{κ^2(N,N′)((ArN)$_2$C−N(H)Ar)}] (Ar = C_6H_4(OMe)−2; **9**).* Complex **9** was prepared from **6** (150 mg, 0.229 mmol) and DMAD (65 mg, 0.457 mmol) in CH_2Cl_2 (10 mL) following the procedure previously described for **8**·H_2O. Complex **9** was purified by crystallization from CH_2Cl_2/*n*-hexane mixture at ambient temperature over a period of 24 h. Yield: 73% (133 mg, 0.167 mmol). IR (KBr, cm^{-1}) ν_{max}: 3322 (w, NH), 1737, 1726 (each s, C═O), 1542 (s, C═N), 1439 (s, N═N), 1237 (s, C−O). ^{1}H NMR (300 MHz, $CDCl_3$, ppm): δ_H = 1.11 (d, $J_{H,H}$ = 6.9 Hz, 6H, CH(CH_3)$_2$), 2.01 (s, 3H, CH_3), 2.53−2.58 (m, 1H, $CHMe_2$), 3.75 (s, 3H, OCH_3), 3.77 (s, 2 × 3H, OCH_3), 3.82 (s, 2 × 3H, OCH_3), 5.28 (apparent q, $J_{H,H}$ = 5.6 Hz, 4H, C_6H_4), 6.28 (br m, 1H, Ar*H*), 6.52 (s, 2H, Ar*H*), 6.61 (d, $J_{H,H}$ = 7.8 Hz, 2H, Ar*H*), 6.74 (t, $J_{H,H}$ = 7.4 Hz, 2H, Ar*H*), 6.83 (t, $J_{H,H}$ = 7.5 Hz, 2H, Ar*H*), 7.01 (d, $J_{H,H}$ = 7.5 Hz, 2H, Ar*H*), 7.22 (d, $J_{H,H}$ = 8.1 Hz, 1H, Ar*H*), 7.36 (s, 1H, N*H*). ^{13}C{^{1}H} NMR (100 MHz, $CDCl_3$, ppm): δ_C = 18.2 (CH_3), 22.2 (CH(CH_3)$_2$), 30.8 ($CHMe_2$), 51.7 (C(O)OCH_3), 55.1, 55.2 (OCH_3), 81.4, 82.4, 96.6, 102.4 (*p*-

dx.doi.org/10.1021/ic201343w | *Inorg. Chem.* 2012, 51, 157−169

cymene ArC), 108.4, 110.4, 119.7, 120.8, 121.1, 121.7, 122.8, 125.0, 127.0 (ArC), 136.9 (C(C(O)OMe)), 139.4, 147.2, 152.0, 155.1 (ArC and C=N), 163.2 (OC(O)). Note: Only 2 carbon resonances were observed for OCH_3 rather than the expected 3 peaks, and 13 carbon resonances were observed for ArC and C=N carbons of the guanidinate ligand rather than the expected 19 peaks, presumably because of overlapping peaks. Anal. Calcd for $C_{38}H_{42}N_6O_7Ru$ (M_w: 795.86): C, 57.35; H, 5.32; N, 10.56. Found: C, 57.12; H, 5.02; N, 10.32.

*[(η^6-$C_{10}H_{14}$)Ru{N_3C_2(C(O)OMe)$_2$}{κ^2(N,N′)((ArN)$_2$C–N(H)Ar)}] (Ar = C_6H_4Me–2; **10**).* Complex **10** was prepared from **7** (200 mg, 0.330 mmol) and DMAD (94 mg, 0.661 mmol) in CH_2Cl_2 (10 mL) following the procedure previously described for **8**·H_2O. Complex **10** was purified by crystallization from CH_2Cl_2/*n*-hexane mixture at ambient temperature over a period of 24 h. Yield: 72% (178 mg, 0.238 mmol). IR (KBr, cm^{-1}) ν_{max}: 3379 (w, NH), 1726 (s, C=O), 1541 (C=N), 1461 (s, N=N), 1223 (s, C–O). The ^{1}H NMR spectrum of **10** revealed the presence of two isomers, but their relative ratios were difficult to estimate because of overlapping peaks (see later). ^{1}H NMR (300 MHz, $CDCl_3$, ppm): δ_H = 1.02 (d, $J_{H,H}$ = 6.3 Hz, CH(CH_3)$_2$, major isomer), 1.12 (br, CH(CH_3)$_2$, minor isomer), 1.80 (br, CH_3), 2.01 (CH_3), 2.06 (CH_3), 2.42 (br, CH_3), 3.86 (s, OCH_3)), 5.25, 5.50 (each br, C_6H_4), 6.67–7.01 (br, ArH), 7.42, 7.81 (ArH and NH). Anal. Calcd for $C_{38}H_{42}N_6O_4Ru$ (M_w: 747.86): C, 61.03; H, 5.66; N, 11.24. Found: C, 60.94; H, 5.24; N, 11.18.

Single Crystal X-ray Structure Determination. Intensity data of suitably sized crystals of **1**, **5**, **6**, and **8**·H_2O were collected on an Oxford Xcalibur S diffractometer (4-circle κ goniometer, Sapphire-3 CCD detector, ω scans, graphite monochromator, and a single wavelength Enhance X-ray source with Mo$K\alpha$ radiation).[27] Pre-experiment, data collection, data reduction and absorption corrections were performed with the CrysAlisPro software suite.[28] Intensity data of suitably sized crystals of **2**–**4** and **10** were collected on a Bruker AXS SMART-APEX diffractometer with a CCD area detector, graphite monochromator.[29] The frames were collected by ω, ϕ, and 2θ rotation at 10 s per frame with SMART. The measured intensities were reduced to F^2 and corrected for absorption with SADABS.[30] The structures were solved by direct methods using SIR 92,[31] which revealed the atomic positions, and refined using the SHELX-97 program package[32] and SHELXL97[33] (within the WinGX program package).[34] Non-hydrogen atoms were refined anisotropically. C–H hydrogen atoms were placed in geometrically calculated positions by using a riding model. The molecular structures were created with the Diamond program.[35] The X-ray crystallographic parameters, details of data collection and structure refinement are presented in Tables 1 and 2.

RESULTS AND DISCUSSION

Synthesis. Complexes **1**–**4** were prepared in high yield from the bridge-splitting reaction involving [(η^6-$C_{10}H_{14}$)RuCl-(μ-Cl)]$_2$ and the respective *N*,*N*′,*N*″-triarylguanidine in toluene in 1:4 mol ratio at ambient temperature for 2 h following the procedure published for **I**.[22] One mole of guanidine was incorporated as a monoanion per ruthenium atom in **1**–**4**, and two moles of guanidine are lost as a guanidinium salt (**C**) in the transformation shown in Scheme 1. The reaction of [(η^6-$C_{10}H_{14}$)RuCl(μ-Cl)]$_2$ with a sterically more hindered $LH_2^{2,6\text{-xylyl}}$ in 1:4 mol ratio in toluene at ambient temperature for 2 h did not afford any new complex.

Complexes **1**–**3** upon reaction with an excess of NaN_3 in ethanol at ambient temperature for 6 h afforded the corresponding azido complexes **5**–**7** in high yield (Scheme 2). Half sandwich ruthenium(II) azido complexes are interesting scaffolds from the point of view of their structures and reactivity pattern, especially [3 + 2] cycloaddition reaction of this class of complexes with nitrile, isonitrile, and alkynes to afford nitrogen bound, carbon bound tetrazolate and nitrogen bound triazolate metal complexes, respectively.[36–46] Hence, complex **5** was treated with diethylacetylenedicarboxylate (DEAD) in CH_2Cl_2 at ambient temperature for 24 h to afford **8**·H_2O in 60% yield. Similarly, **6** and **7** upon reaction with dimethylacetylenedicarboxylate (DMAD) in CH_2Cl_2 at ambient temperature afforded **9** and **10** in 73 and 72% yield, respectively (Scheme 3). Complexes **5**–**7** were also treated with electron rich methylphenyl propiolate and diphenyl acetylene separately in CH_2Cl_2 at ambient temperature for 24 h, but no new products were isolated from these reactions.

Scheme 1

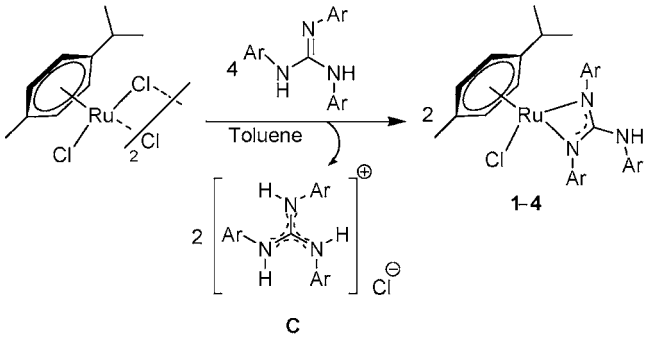

	Ar	Yield (%)
1	C_6H_4Me–4	90
2	C_6H_4(OMe)–2	95
3	C_6H_4Me–2	92
4	$C_6H_3Me_2$–2,4	79

Scheme 2

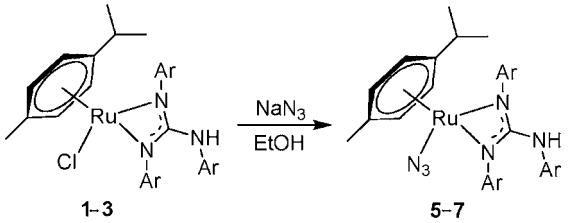

	Ar	Yield (%)
5	C_6H_4Me–4	82
6	C_6H_4(OMe)–2	82
7	C_6H_4Me–2	94

Scheme 3

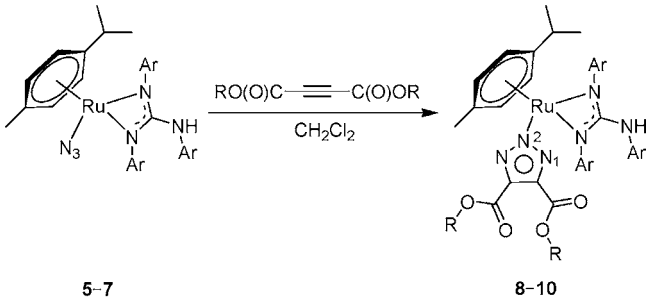

	R	Ar	Yield (%)
8	Et	C_6H_4Me–4	60
9	Me	C_6H_4(OMe)–2	73
10	Me	C_6H_4Me–2	72

dx.doi.org/10.1021/ic201343w | *Inorg. Chem.* 2012, 51, 157–169

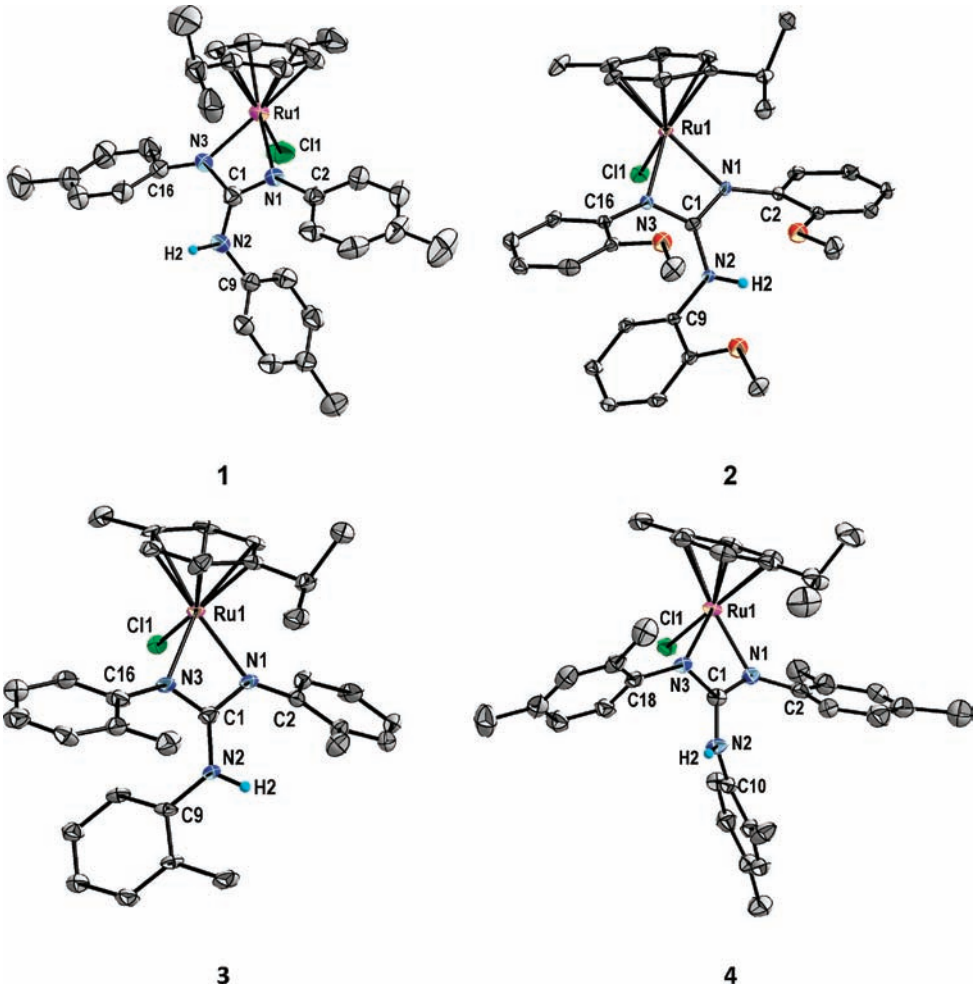

Figure 1. Molecular structures of **1**–**4** at the 50% probability level. Two molecules crystallized in an asymmetric unit in the case of **2**, but only molecule 1 is shown for clarity. Only the hydrogen atom of the amino moiety is shown for clarity.

Molecular Structures. The molecular structures of **1**–**4** with atom labeling schemes are shown in Figure 1. Selected bond parameters are listed in Table 3. The ruthenium atom in **1**–**4** is surrounded by the η^6-bonded *p*-cymene ring, a chelating *N,N′,N″*-triarylguanidinate ligand, and the chloride and thus attains a pseudo octahedral "three legged piano stool" geometry; the *p*-cymene ring constitutes a seat, the chloride and two nitrogen atoms of the guanidinate ligand constitute three legs. The structural features of **1**–**4** are listed in Table S1 in the Supporting Information.

In principle, four resonance forms, **D**–**G**, can be drawn for the ruthenium bonded guanidinate ligand as illustrated in Chart 2. An equal contribution of resonance forms **D** and **E** would result in the π–delocalized form **F** and a symmetric coordination of the nitrogen atoms of the guanidinate ligand. The magnitude of Δ_{CN} (= d(C–N) − d(C═N)) and Δ_{CN}' (= d(C–N(H)) − d(C═N))[25,47] gives an insight regarding the relative contribution of a particular resonance form to the overall structure and bonding of amidinate and guanidinate complexes. The Δ_{CN} values range from 0 Å in a π–delocalized form **F** up to 0.10 Å in the π–localized forms **D** and **E** retaining the C–N single bond and the C═N double bond character. The zwitterionic form **G** would be feasible when τ(N–C–N(H)–C) torsion angle is close to 0 or 180° and when the N(H)R nitrogen is sp^2 hybridized and planar. Further, the dihedral angle between the NCN plane of the chelate ring and that of the NHC(R) unit should be close to zero.[20c,48]

In general, the Δ_{CN} value is smaller than the Δ_{CN}' value for **1**–**4** (Δ_{CN}; Δ_{CN}': 0.013(6); 0.059(6) (**1**), 0.009(6); 0.056(6) (**2**; molecule 1), 0.001(9); 0.042(8) (**3**), and 0.007(6); 0.056(6) (**4**)) indicating a better alignment of the N_{coord}Ar lonepair than the NHAr lonepair with C═Nπ* orbital of the imine unit. The CN_3 carbon of the guanidinate ligand is planar. The nitrogen atoms in **1**–**3** are planar ($\sum$N ≈ 360°) or nearly planar ($\sum$N ≈ 354–358°). However, one of coordinated nitrogen atoms in **4** significantly deviates from planarity ($\sum$N: 348.6°), and the remaining nitrogen atoms are planar or nearly planar ($\sum$N: 356.8°). A slightly pyramidal geometry ($\sum$N: 355.5°) of one of the coordinated nitrogen atoms and a comparable Ru–N distances (2.098(2) and 2.105(2) Å) in **1** or a planar geometry of the coordinated nitrogen atoms and an unequal Ru–N distances (2.107(3), and 2.086(3) Å) in **2** (molecule 1) or a slightly pyramidal geometry ($\sum$N: 353.8°) of one of the coordinated nitrogen atoms and unequal Ru–N distances (2.125(4) and 2.093(4) Å) in **3** support unequal contributions of forms **E** and **F**. A nonplanar geometry of the coordinated nitrogen atoms and unequal Ru–N distances (2.105(3) and 2.149(3) Å) in **4** indicate unequal contributions of forms **D** and **E**. The N–C–N(H)–C torsion angles in **4** (−42.9(5) and 140.0(4)°) deviate from 0 or 180° to a greater extent than those found in **3** (23.4(10) and −153.8(5)°).

dx.doi.org/10.1021/ic201343w | *Inorg. Chem.* 2012, 51, 157–169

Table 3. Selected Bond Distances (Å) and Angles (deg) for 1−4

	1	2 (molecule 1)	3	4
Ru1−C(centroid)	1.6648(8)	1.6526(4)	1.652(1)	1.6620(3)
Ru1−N1	2.098(2)	2.107(3)	2.125(4)	2.105(3)
Ru1−N3	2.105(2)	2.086(3)	2.093(4)	2.149(3)
Ru1−Cl1	2.410(1)	2.411(1)	2.412(2)	2.397(9)
N1−C1	1.319(4)	1.333(4)	1.331(7)	1.320(5)
N2−C1	1.378(4)	1.380(4)	1.372(6)	1.376(4)
N3−C1	1.332(4)	1.324(4)	1.330(6)	1.327(4)
N1−C2	1.402(4)	1.401(4)	1.423(7)	1.406(5)
N2−C9/N2−C10	1.422(4)	1.420(4)	1.421(7)	1.436(4)
N3−C16/N3−C18	1.409(4)	1.400(4)	1.404(6)	1.422(5)
Ru1−N1−C2	135.1(2)	137.1(2)	135.7(3)	134.6(2)
C2−N1−C1	130.2(3)	128.8(3)	125.5(4)	127.9(3)
Ru1−N1−C1	94.6(2)	94.0(2)	92.6(3)	94.3(2)
C9−N2−C1/C10−N2−C1	124.3(2)	124.5(3)	126.7(4)	122.4(3)
C1−N2−H2	117.9(3)	117.7(3)	116.6(4)	118.7(3)
C9−N2−H2/C10−N2−H2	117.8(2)	117.7(3)	116.6(4)	118.9(3)
Ru1−N3−C16/Ru1−N3−C18	135.4(2)	136.5(2)	134.0(3)	134.4(2)
C16−N3−C1/C18−N3−C1	126.3(3)	127.9(3)	131.9(4)	122.1(3)
Ru1−N3−C1	93.8(2)	95.2(2)	94.1(3)	92.1(2)
N1−C1−N2	126.6(3)	122.0(3)	123.7(5)	125.7(3)
N2−C1−N3	124.8(3)	129.4(3)	126.8(5)	123.3(3)
N3−C1−N1	108.6(3)	108.5(3)	109.4(4)	111.0(3)
Cl1−Ru1−N3	87.51(8)	85.6(1)	85.6(1)	86.08(8)
Cl1−Ru1−N1	85.63(8)	87.6(1)	87.8(1)	85.40(9)
N1−Ru1−N3	61.57(9)	61.9(1)	62.0(2)	61.7(1)

Chart 2. Limiting Resonance Forms of 1−4[a]

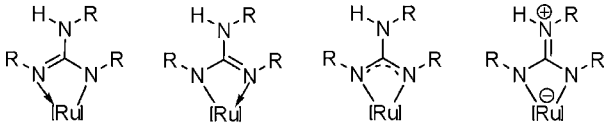

[a][Ru]: (η^6-*p*-cymene)RuCl.

Further, the dihedral angle between the HNC(Ar) plane and the chelate NCN plane is greater in **4** (41.4(3)°) than in **3** (25.0(5)°), possibly because of a greater pyramidal geometry of one of the coordinated nitrogen atoms in the former, and this in turn arises because of the greater donor strength of xylyl substituent in **4** than tolyl substituent in **3**. The RuNCN chelate ring in **3** is more puckered than that in **4**. This feature is counterintuitive as one of the coordinated nitrogen atoms is more pyramidal in the latter, but this appears to arise from the difference in the conformation of the guanidinate ligand in these complexes (see later).

The *o*-substituent of the aryl ring of the coordinated nitrogen atoms can lie parallel (i.e, *syn*) or anti parallel (i.e, *anti*) to the corresponding substituent of the aryl ring of the non-coordinated nitrogen atom of the guanidinate ligand in **2**−**4**. Thus, *syn-syn*, *syn-anti*, *anti-syn*, and *anti-anti* conformations are possible for **2**−**4**, as illustrated in Figure 2.[49] Accordingly, the guanidinate ligand in **2** (molecule 1) and **3** adopts *syn-syn* conformation while that in **4** adopts *syn-anti* conformation with some distortion in the crystal lattice.

Guanidines $LH_2^{2\text{-tolyl}}$ and $LH_2^{2,4\text{-xylyl}}$ were shown to possess *anti-anti* $\alpha\beta\alpha$ conformation whereas $LH_2^{2\text{-anisyl}}$ was shown to possess *syn-anti* $\alpha\beta\beta$ conformation in the crystal lattice.[24] Thus, the difference in conformation of the guanidinate ligand in **3**

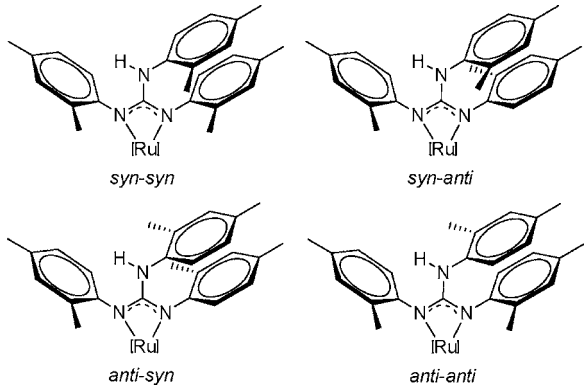

Figure 2. Four possible conformations of **2**, **3**, and **4**. The substituent symbol on the aryl rings of the guanidinate ligand is omitted for clarity. [Ru]: (η^6-*p*-cymene)RuCl.

and **4** does not appear to originate from the conformational difference between two guanidines from which these complexes were obtained. A hypothetical *syn-syn* isomer of **4** is possibly a kinetically controlled isomer of the bridge splitting reaction shown in Scheme 1 and rearranges to a thermodynamically controlled *syn-anti* isomer via an intermediate **H** shown in Figure 3 because of a greater steric strain present in the former isomer induced by a greater pyramidal geometry of one of the coordinated nitrogen atoms. The rearrangement shown in Figure 3 bears some resemblance to the rearrangement that follows insertion of *N*,*N*′-diisopropylcarbodiimide into Ln−N bond.[50]

The molecular structures of **5** and **6** are illustrated in Figure 4. Selected bond parameters are listed in Table 4. The coordination environment and bond parameters around the ruthenium atom in **5** and **6** are nearly identical to those found in **1** and **2**, respectively, except that the chloride in the latter

dx.doi.org/10.1021/ic201343w | *Inorg. Chem.* 2012, 51, 157−169

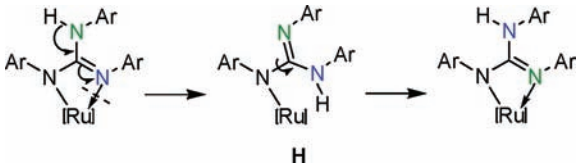

Figure 3. Guanidine centered rearrangement of **4** illustrating amine-imine tautomerization, ring-opening, C−N bond rotation, and ring closing events. [Ru]: (η^6-*p*-cymene)RuCl.

complexes is substituted by the azide in the former. The degree of n−π conjugation within the RuNCN chelate ring (Δ_{CN}; Δ_{CN}': 0.021(6); 0.048(6) (**5**), and 0.011(4); 0.040(5) (**6**)) is greater. The perusal of Δ_{CN} values, angle sums around the nitrogen atoms (∑N1: 353.0°, ∑N2, N3: 360.0° (**5**); ∑N1: 359.8°, ∑N2: 360.0° and ∑N3: 358.1° (**6**)) and Ru−N distances (Ru1−N1/Ru1−N3: 2.103(2)/2.125(3) Å (**5**); 2.080(2)/2.108(2) Å (**6**)) indicate a major contribution of form **D** to the bonding of **5** whereas forms **E** and **F** contribute unequally to the bonding of **6**. The guanidinate ligand in **6** is shown to reveal *syn-syn* conformation. The azido ligand in **5** and **6** adopts an end-on terminal coordination mode, and the bond parameters associated with this ligand are comparable with those reported for [[(η^6-$C_{10}H_{14}$)RuN_3\{κ^2(*N*,*N*′)(5-(4-nitrophenyl)dipyrromethene)\}] (**III**).[51]

The molecular structures of **8**·H_2O and **10** are illustrated in Figure 5. Selected bond parameters are listed in Table 5. The ruthenium atom in **8**·H_2O and **10** is surrounded by the η^6-bonded *p*-cymene ring, two nitrogen atoms of *N*,*N*′,*N*″-triarylguanidinate ligand and the central nitrogen atom of the triazolate ring (i.e., N2 bonded isomer) and thus revealed a pseudo octahedral "three legged piano stool" geometry. The Δ_{CN}: 0.004(4) Å value is smaller than Δ_{CN}': 0.038(4) Å value for the guanidinate ligand in **8**·H_2O. However, Δ_{CN} and Δ_{CN}' values in **10** are comparable within the experimental uncertainties (Δ_{CN}: 0.001(10) Å; Δ_{CN}': 0.021(10) Å), possibly because of an improved n−π conjugation involving the NHAr lone pair with the C═Nπ* orbital of the imine unit. The greater n−π conjugation in **10** than in **8**·H_2O is due to greater π−acceptor character of the ruthenium atom caused by the less strongly donating and more sterically encumbered *o*-tolyl moiety of the guanidinate ligand in the former. One of the coordinated nitrogen atoms in **8**·H_2O is more pyramidal than the other (∑N: 347.7 and 359.1°) because of the presence of more strongly donating *p*-tolyl substituent, but both coordinated nitrogen atoms in **10** are nearly planar (∑N: 356.9 and 354.6°). The noncoordinated nitrogen atoms in **8**·H_2O and **10** are planar. The Ru(1)−N(1) distance, 2.089(2) Å in **8**·H_2O, is slightly smaller than the Ru(1)−N(3) distance, 2.140(2) Å, but the bond distance difference is smaller in **10** (2.088(5) versus 2.104(4) Å). Thus, forms **D** and **F** appear to contribute unequally to the bonding of the guanidinate ligand in **8**·H_2O whereas forms **D**, **E**, and **F** contribute to different extent to the bonding of the same ligand in **10**.

The guanidinate ligand in **10** possesses *syn-anti* conformation in contrast to *syn-syn* conformation observed for the same ligand in **3** and presumably in **7**. The greater steric encumbrance around the ruthenium atom in a hypothetical *syn-syn* isomer of **10** as compared with that found in **3** or **7** probably facilitates the guanidine centered rearrangement such as that shown in Figure 3 and during such rearrangement the guanidinate ligand rearranges to a sterically less encumbered *syn-anti* conformation.

Spectroscopic Properties. The IR spectrum of **1** and **3**−**10** revealed one band in 3295−3435 cm^{-1} region attributed to the ν(NH) stretch. However, the IR spectrum of **2** revealed two bands at 3419 and 3330 cm^{-1} attributed to the ν(NH) stretch of two distinct molecules in the crystal lattice. Complexes **5**−**7** also revealed a new band at 2030, 2026, and 2028 cm^{-1}, respectively attributed to the $\nu(N_3)$ stretch, and values of these bands favorably matched with that reported for the related half-sandwich ruthenium(II) azido complexes.[36−44] Complexes **8**·H_2O and **9** revealed two bands (1710 and 1725 cm^{-1} (**8**·H_2O); 1726 and 1737 cm^{-1} (**9**)), but complex **10** revealed one band at 1726 cm^{-1} attributed to the ν(C═O) stretch of the ester group. The presence of one water molecule in the crystal lattice of **8** was confirmed by microanalytical data. Further, the TGA thermogram of **8**·H_2O revealed 2.53% weight loss (theoretical weight loss: 2.27%) in the temperature range 45−139.26 °C indicating the loss of one water molecule. The water loss was also confirmed by a DTA experiment that revealed a sharp endotherm at 139.26 °C (Figure S4 in the Supporting Information).

Complex **3** was subjected to a VT ^{1}H NMR study to understand its fluxional behavior. The ^{1}H NMR stack plot for alkyl protons as a function of temperature is illustrated in

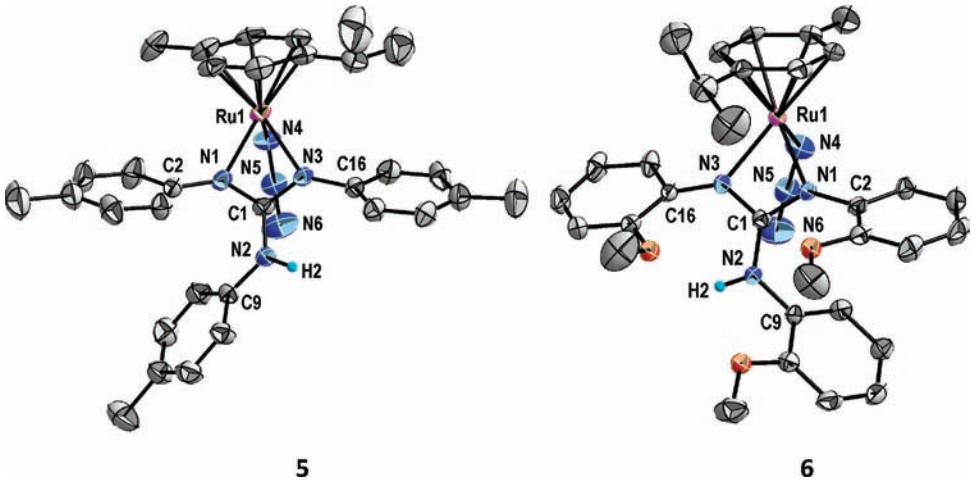

Figure 4. Molecular structures of **5** and **6** at the 50% probability level. Only the hydrogen atom of the amino moiety is shown for clarity.

dx.doi.org/10.1021/ic201343w | *Inorg. Chem.* 2012, 51, 157−169

Table 4. Selected Bond Distances (Å) and Angles (deg) for 5 and 6

	5	6		5	6
Ru1−C(centroid)	1.6767(2)	1.6635(3)	N3−C1	1.321(4)	1.340(3)
Ru1−N1	2.103(2)	2.080(2)	N1−C2	1.398(4)	1.401(4)
Ru1−N3	2.125(3)	2.108(2)	N2−C9	1.412(4)	1.402(4)
Ru1−N4	2.121(3)	2.116(3)	N3−C16	1.400(4)	1.383(4)
N1−C1	1.342(4)	1.329(3)	N4−N5	1.197(4)	1.184(4)
N2−C1	1.369(4)	1.369(4)	N5−N6	1.149(4)	1.151(4)
Ru1−N1−C2	129.7(2)	132.8(2)	C16−N3−C1	129.6(3)	130.7(3)
C2−N1−C1	128.2(3)	131.3(3)	N1−C1−N2	126.2(3)	128.6(3)
Ru1−N1−C1	95.1(2)	95.7(2)	N2−C1−N3	125.2(3)	123.7(3)
C9−N2−C1	126.1(3)	125.0(3)	N3−C1−N1	108.6(3)	107.6(3)
C1−N2−H2	117.0(3)	117.5(3)	N1−Ru1−N3	61.5(1)	61.9(9)
C9−N2−H2	116.9(3)	117.5(3)	N3−Ru1−N4	87.0(1)	89.0(1)
Ru1−N3−C16	135.6(2)	133.3(2)	N4−Ru1−N1	86.8(1)	86.2(1)
Ru1−N3−C1	94.8(2)	94.1(2)	N4−N5−N6	177.8(4)	175.5(4)

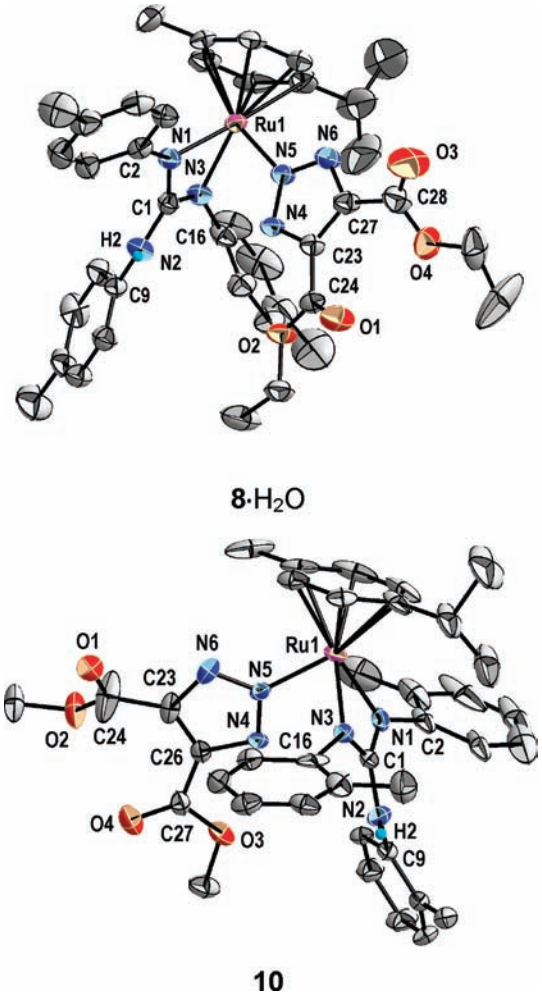

Figure 5. Molecular structures of **8**·H_2O and **10** at the 50% probability level. The lattice water molecule is omitted for clarity in the case of **8**·H_2O. The O1 atom in **10** is disordered over three sites, but only one site is shown for clarity. Only the hydrogen atom of the amino moiety is shown for clarity.

Figure 6. At 313 K, an intense doublet was observed at δ_H = 1.18 ppm ($J_{H,H}$ = 6.8 Hz) accompanied by a minor doublet at δ_H = 1.24 ppm ($J_{H,H}$ = 7.2 Hz) in about 6.5:1 ratio assignable to $CH(CH_3)_2$ protons, and the former doublet gradually broadens upon lowering the temperature and merges with the latter at 283 K. Upon further cooling to 253 K, three distinct signals appeared at δ_H = 1.06 (br), 1.16 (d, $J_{H,H}$ = 6.8 Hz), and 1.30 (br) ppm. The inner and outer broad peaks became a doublet ($J_{H,H}$ = 6.4 and 6.8 Hz) upon further lowering the temperature. At temperatures ≤233 K, the ^{1}H NMR spectra revealed three well-defined doublets at δ_H = 1.04, 1.21, and 1.34 ppm ($J_{H,H}$ = 6.8 Hz) in about 1:1:1 ratios indicating the presence of three isomers in solution. The perusal of a VT ^{1}H NMR pattern of the *p*-cymene ring protons further confirmed the presence of three isomers at temperatures ≤253 K (Figure S5 in the Supporting Information).

Two-dimensional ^{1}H−^{1}H COSY NMR data was acquired for **3** at 233 K to gain an insight concerning the orientation of the *p*-cymene ring with respect to the Ru−N and Ru−Cl bond axes. The three pairs of off-diagonal peaks observed between $CH(CH_3)_2$ protons and guanidinate *o*-CH_3 protons of the coordinated nitrogen atoms clearly indicated the proximity of these two units in solution (Figure S6, inset a in the Supporting Information). Of the three doublets observed for $CH(CH_3)_2$ protons, the inner and outer doublets are assigned to two symmetric isomers, and the central doublet is assigned to a less symmetric isomer based on the ^{1}H−^{1}H COSY NMR pattern illustrated in Figure S6, inset a, in the Supporting Information as well as from the growth pattern of these peaks illustrated in Figure 6. The ^{1}H−^{1}H COSY NMR pattern of the *p*-cymene ring protons also revealed the presence of two symmetric isomers and one less symmetric isomer (Figure S6, inset b, in the Supporting Information). The DEPT-90 ^{13}C NMR spectrum of **3** measured at 233 K revealed six signals at δ_C = 77.8, 78.0, 78.2, 78.4, 80.5, and 82.0 ppm attributed to the CH carbon of the *p*-cymene ring, and this spectral pattern further confirmed the presence of three isomers in solution (Figure S7 in the Supporting Information).

The *p*-cymene ring in [(η^6-*p*-cymene)RuX(NN)] (NN: monoanionic bidentate *N*-donor ligand; X = Cl or N) can orient in six different eclipsed conformations around the ruthenium atom such as **I**−**N** (Figure S8 in the Supporting Information). In addition, several staggered conformations are also possible. The preference of a particular conformer of [(η^6-*p*-cymene)RuCl(NN)]$^+$X$^-$ was shown to depend largely upon the steric bulk of the substituents on the nitrogen atom.[52−57] Further, various conformers of [(η^6-*p*-cymene)Ru(ethylenediamine)Cl]$^+$ were shown to differ in energy by ≤2

dx.doi.org/10.1021/ic201343w | *Inorg. Chem.* 2012, 51, 157−169

Table 5. Selected Bond Distances (Å) and Angles (deg) for 8·H_2O and 10

	8·H_2O	10		8·H_2O	10
Ru1−C(centroid)	1.6753(5)	1.6746(6)	C(1)−N(1)−C(2)	128.0(2)	128.4(5)
Ru(1)−N(1)	2.089(2)	2.088(5)	C(2)−N(1)−Ru(1)	135.9(2)	133.8(4)
Ru(1)−N(3)	2.140(2)	2.104(4)	C(1)−N(2)−H(2)	116.3(2)	116.3(5)
Ru(1)−N(5)	2.106(2)	2.102(4)	C(1)−N(2)−C(9)	127.5(2)	127.5(5)
N(1)−C(1)	1.330(3)	1.330(7)	C(9)−N(2)−H(2)	116.2(3)	116.2(5)
N(2)−C(1)	1.368(3)	1.351(7)	C(1)−N(3)−Ru(1)	92.8(2)	94.0(3)
N(3)−C(1)	1.334(3)	1.331(7)	C(16)−N(3)−Ru(1)	129.6(2)	133.8(4)
N(4)−N(5)	1.320(3)	1.340(6)	C(16)−N(3)−C(1)	125.3(2)	126.8(4)
N(5)−N(6)	1.341(3)	1.328(6)	N(4)−C(23)−C(27)/N(6)−C(23)−C(26)	107.8(2)	108.2(5)
N(2)−C(1)−N(3)	127.5(2)	123.4(5)	N(5)−N(6)−C(27)/N(5)−N(4)−C(26)	105.1(2)	105.4(4)
N(3)−C(1)−N(1)	108.5(2)	108.6(4)	N(4)−N(5)−N(6)	112.7(2)	112.7(4)
N(1)−C(1)−N(2)	124.0(2)	128.0(5)	N(5)−N(4)−C(23)/N(5)−N(6)−C(23)	106.1(2)	105.9(4)
C(1)−N(1)−Ru(1)	95.2(2)	94.7(3)	N(4)−C(23)−C(27)/N(4)−C(26)−C(23)	107.8(2)	107.7(5)

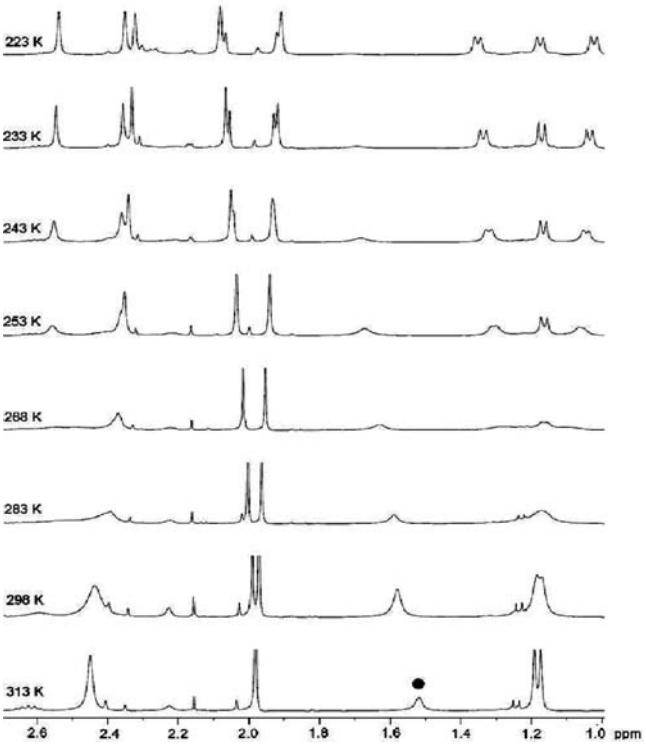

Figure 6. VT ^{1}H NMR spectrum (400 MHz, CD_2Cl_2) of **3** for the alkyl protons. The • symbol indicates adventitious proton signal of H_2O.

kcal/mol.[58] Thus, complex **3** appears to exist as conformer **I** wherein the ^{i}Pr moiety of the *p*-cymene ring resides exactly between *o*-Me substituent of two $N_{coord}Ar$ moieties, and the guanidinate ligand appears to exist in *syn-syn* conformation as found in the solid state.

Half-sandwich ruthenium(II) complexes of the type $[(\eta^6\text{-}C_{10}H_{14})RuCl(EE')]^{n+}$ (EE′: monoanionic bidentate oxygen, and nitrogen donor ligand or neutral bidentate oxygen and nitrogen donor ligand; n = 0 or 1)[2a,11,53a,55,59−61] were shown to reveal a pair of doublets for $CH(CH_3)_2$ protons and two pairs of doublets for the *p*-cymene ring protons, and this spectral pattern was ascribed to the presence of two diastereomers that stems from chirality of the ruthenium atom. The ruthenium atom in **1** and **2** appears to be achiral as only one doublet was observed for $CH(CH_3)_2$ protons and only a pair of doublet was observed for the *p*-cymene ring protons. Hence, the chiral at ruthenium option is ruled out for **1**−**4**.

$[ML_2\{\kappa^2(N,N')((i\text{PrN})_2C\text{−}NR_2\}_2]$ [M = Ti; L = Cl, R = Me (**IV**);[62] M = Hf; L = NEt_2; R = Et (**V**)[63]] and a homoleptic $[Ga\{\kappa^2(N,N')((i\text{PrN})_2C\text{−}NR_2\}_3]$ (R = Me; **VI**[48a]) were shown to undergo N−$CHMe_2$ bond rotation or C−NR_2 bond rotation along the guanidinate C_2 axis but the latter process appears to be feasible in **3** for steric reason. Complex **3** in conformation **I** can have three different ligand conformations, namely, *syn-syn* illustrated in Figure 2, *syn-syn a*, and *syn-syn b* illustrated in Chart 3. The *syn-syn* ↔ *syn-syn a* or *syn-syn a* ↔ *syn-syn b*

Chart 3. Plausible Structures of Two Rotamers of 3[a]

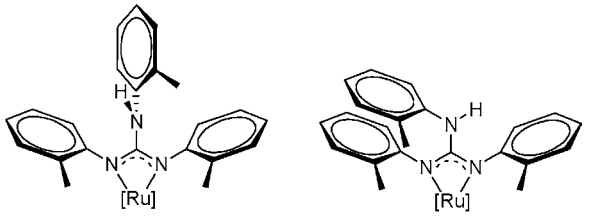

syn-syn a *syn-syn b*

[a][Ru]: (η^6-*p*-cymene)RuCl.

interconversion requires 60° C−N(H)(*o*-tolyl) bond rotation in a region away from the *o*-Me protons of the *o*-tolyl moiety of the coordinated nitrogen atoms to minimize the unfavorable steric repulsion. A complete 180° C−N(H)(*o*-tolyl) bond rotation would convert *syn-syn* conformer to *anti-anti* conformer, but this process appears to be unfavorable because of the repulsive interaction between the bulky *o*-tolyl moiety of the coordinated nitrogen atoms with that of the noncoordinated nitrogen atom. In solution, the three conformers or more precisely the three rotamers of **3** are in rapid equilibrium at ambient temperature because of the fast C−N(H)Ar bond rotation, but upon lowering the temperature, C−N(H)Ar bond rotation is slowed down because of the presence of a bulky *o*-tolyl substituent of the guanidinate ligand and occurs at a rate comparable with the NMR time scale.

That the three isomers of **3** in solution arise from the C−N(H)Ar bond rotation rather than from the guanidine centered rearrangement illustrated in Figure 3 gains further support from the following points. (i) The C−N(H)Ar distance, 1.372(6) Å in **3** indicates a single bond character and the N(H)Ar nitrogen is planar. (ii) The energy requirement for ligand dissociation of

dx.doi.org/10.1021/ic201343w | *Inorg. Chem.* 2012, 51, 157−169

a coordinatively saturated low-spin d^6 complex of a second or third row transition metals is rather high (ΔG^*) 25 kcal/mol).[64] (iii) Guanidine centered rearrangement converts a more symmetric *syn-syn* conformer to a less symmetric *syn-anti* conformer, but the observed solution conformation is **I** wherein the guanidinate ligand is shown to adopt *syn-syn* conformation (see above).

Complex **2** was also subjected to a VT ^{1}H NMR study under the condition identical to that mentioned previously for **3** (Figure S9 in the Supporting Information). However, no noticeable change was observed in the ^{1}H NMR pattern of both alkyl and aryl protons throughout the temperature range studied. The presence of less bulky *o*-anisyl substituent in **2** than the *o*-tolyl substituent in **3** permits a fast C−N(H)Ar bond rotation in the former, and the rate of this process appears to be greater than the NMR time scale even at low temperatures studied. Moreover, the void space encircled by *o*-OMe substituent in **2** is greater than that encircled by the *o*-Me substituent in **3** (Figure S10 in the Supporting Information). The ^{1}H NMR spectrum of **2** revealed the presence of three rotamers in about 1.0:0.05:0.04 ratios in CD_3CN as estimated from the integrals of C*H* protons of the *p*-cymene ring. Perhaps, the N*H*Ar proton in **2** is involved in intermolecular N−H···N hydrogen bonding with CD_3CN, and this would make the NHAr nitrogen more pyramidal resulting in the restricted C−NH(Ar) bond rotation even at ambient temperature. The influence of CD_3CN upon the number of rotamers of fluorinated hydrazone is reported in the literature.[65]

The ^{1}H NMR spectrum of **4** in $CDCl_3$ revealed the presence of three isomers in about 1.0:1.1:3.8 ratios as estimated from the integrals of $CH(CH_3)_2$ protons, and these three isomers are assigned to *syn-syn*, *syn-syn a*, and *syn-syn b* isomers as discussed previously for **3**. Probably, complexes such as **3** and **4** possess only three rotatable N_{coord}−C−N(H)−C(Ar) torsion angles largely because of the steric constraint imposed by the *o*-Me substituent of the guanidinate ligand. The barrier for the C−N bond rotation was shown to be sufficient enough for the isolation of rotamers of amides with bulky *o*-substituted aryl groups.[66]

The ^{1}H and ^{13}C NMR data of **5**, **6**, **8**·H_2O, and **9** in $CDCl_3$ revealed the presence of only one isomer because of the presence of less bulky *p*-tolyl substituent in **5** and **8**·H_2O and *o*-anisyl substituent in **6** and **9** that permit a simultaneous and fast C−N(H)Ar and ruthenium−arene(centroid) bond rotations, and the rate of these processes appears to be greater than the NMR time scale. In principle, [3 + 2] cycloaddition reaction of metal azido complexes with alkynes can give either N1 (or terminal nitrogen) or N2 (or central nitrogen) bonded metal triazolate isomers or only N2 bonded metal triazolate isomer. It has been suggested that the N1 bonded triazolate isomer is a kinetically controlled product while the N2 bonded triazolate isomer is a thermodynamically controlled product.[67] The transient formation of both the N(1) and N(2) bonded isomers and their subsequent conversion to N(2) bonded isomer of ruthenium(II) triazolate complex was detected by ^{31}P NMR spectroscopy.[37,44] The molecular structures of two N(1) bonded ruthenium(II) triazolate complexes have been reported in the literature.[42] The ^{1}H NMR data of **8**·H_2O and **9** revealed only one type of signal for C(O)OCH_2CH_3 and C(O)OCH_3 protons, respectively, and thus suggested the presence of N2 bonded isomer in solution as well. The N2 bonded isomer of **8**·H_2O, **9**, and **10** could be the thermodynamic products, probably formed via the N1 bonded kinetic products of [3 + 2] cycloaddition reaction.

The ^{1}H NMR spectrum of **10** revealed broad peaks for alkyl/aryl protons, and hence the sample was subjected to a VT ^{1}H NMR study (Figure S11 in the Supporting Information). At 233 K, five closely spaced doublets were observed at δ_H = 0.99, 1.06, 1.10, 1.13, and 1.24 ppm in about 1.0:1·2:2·7:3·5:6·9 ratios assignable to the $CH(CH_3)_2$ protons (Figure S12 in the Supporting Information). The five species could possibly be assigned to any three conformers from **I**−**L** shown in Figure S8 in the Supporting Information with one of them exhibiting a restricted C−N(H)Ar bond rotation as previously discussed for **3**. Although the guanidinate ligand in **4** and **10** revealed *syn-anti* conformation in the solid-state, these complexes differ in the number of solution species, possibly because of the bulkier triazolate ring in the latter complex that permits both the restricted ruthenium-arene(centroid) and C−N(H)Ar bond rotations (Figure S13 in the Supporting Information). The driving force for the fluxional behavior of **3** and **10** is the steric overload caused by either the guanidinate ligand conformation or the substituents around the ruthenium atom or both as has been shown for [PtMe{κ^2(*N*,*N*′)(dmphen)}{P(2-MeO-C_6H_4)$_3$}]SbF_6·H_2O [dmphen: 2,9-dimethyl-1,10-phenanthroline].[68] Thus, it is clear that the number of rotamers in solution depends upon ligand conformation which in turn depends upon the bulkiness of the aryl moiety of the guanidinate ligand. Further, a caveat has appeared sometime ago detailing the presence of two diastereomers for a chiral complex that stems from ligand conformation rather than from epimeric chiral metal center.[69]

CONCLUSIONS

Half sandwich ruthenium guanidinate complexes of the types [(η^6-$C_{10}H_{14}$)RuX(NN)] and [(η^6-$C_{10}H_{14}$)Ru{N_3C_2(C(O)-OR)$_2$}(NN)] (X = Cl and N_3; NN = chelating *N*,*N*′,*N*″-triarylguanidinate ligand; R = Me or Et) were isolated in moderate to high yield, and eight of them were structurally characterized. The *syn-syn* isomer of **3** was invoked as a kinetic product while the *syn-anti* isomer of **4** was invoked as a thermodynamic product of the bridge splitting reaction. The *syn-anti* isomer of **10** and **8**·H_2O with N2 bonded triazolate ring was suggested as a thermodynamic isomer of [3 + 2] cycloaddition reaction. The ruthenium(II) *N*,*N*′,*N*″-tri(*o*-substituted aryl)guanidinate complexes revealed ligand centered stereochemistry both in the solid-state and in solution. The substitution pattern, donor property, and steric bulk of the aryl moiety of the guanidinate ligand dictate the degree of n−π conjugation between the NHAr/N_{coord}Ar lone pair and the C=Nπ* orbital of the imine unit. In solution, **3** and **4** exist as a mixture of three rotamers at temperatures ≤253 K and ambient temperature, respectively, whereas **1** and **2** exist as a single isomer. Thus, the barrier height for the C−N(H) bond rotation appears to decrease in the following order: **4** > **3** ≫ **1**, and **2**. The donor property of the aryl ring of the guanidinate ligand dictates the nature of the conformer in the solid-state whereas the steric property appears to dictate the number of conformers in solution. To some extent, the donor property of the solvent also influences the number of rotamers in solution. The greater number of rotamers in the case of **10** as compared with **4** not only arises because of steric factor associated with *o*-tolyl moiety of the guanidinate ligand but also appears to arise from the steric encumbrance caused by the substituents around the ruthenium atom in the former.

dx.doi.org/10.1021/ic201343w | *Inorg. Chem.* 2012, 51, 157−169

■ ASSOCIATED CONTENT

Supporting Information

X-ray crystallographic data in CIF format, ^{1}H, $^{13}C\{^{1}H\}$, 2D HETCOR NMR of **2** in CD_3CN, Table S1, TGA-DTA thermogram of **8**·H_2O, a VT ^{1}H NMR stack plots of **2**, **10** and that of **3** for the *p*-cymene ring protons, a two-dimensional $^{1}H-^{1}H$ COSY, DEPT-90 ^{13}C NMR spectra of **3**, space-filling views of **2**, **3**, and **10**. This material is available free of charge via the Internet at http://pubs.acs.org.

■ AUTHOR INFORMATION

Corresponding Author

*E-mail: tnat@chemistry.du.ac.in, thirupathi_n@yahoo.com.

■ ACKNOWLEDGMENTS

The Department of Science and Technology, New Delhi, is gratefully acknowledged for the research grant (SR/S1/IC−22/2004 and SR/S1/IC−04/2010). The authors thank the NMR Research Centre, Indian Institute of Science, Bangalore 560 012, for VT ^{1}H NMR measurements and University Science Instrumentation Center, University of Delhi, Delhi 110 007, for NMR, microanalytical, and single crystal X-ray diffraction data for some complexes. Prof. U. P. Singh, Department of Chemistry, Indian Institute of Technology Roorkee, Roorkee 247 667, is gratefully acknowledged for X-ray diffraction data of **2**−**4**, and **10**.

■ REFERENCES

(1) (a) Ikariya, T. *Bull. Chem. Soc. Jpn.* **2011**, *84*, 1−16. (b) Ikariya, T.; Gridnev, I. D. *Chem. Rec.* **2009**, *9*, 106−123. (c) Ikariya, T.; Blacker, A. *J. Acc. Chem. Res.* **2007**, *40*, 1300−1308. (d) Ikariya, T.; Murata, K.; Noyori, R. *Org. Biomol. Chem.* **2006**, *4*, 393−406. (e) Noyori, R.; Hashiguchi, S. *Acc. Chem. Res.* **1997**, *30*, 97−102.

(2) (a) van Rijt, S. H.; Hebden, A. J.; Amaresekera, T.; Deeth, R. J.; Clarkson, G. J.; Parsons, S.; McGowan, P. C.; Sadler, P. J. *J. Med. Chem.* **2009**, *52*, 7753−7764. (b) Meggers, E.; Atilla-Gokcumen, G. E.; Gründler, K.; Frias, C.; Prokop, A. *Dalton Trans.* **2009**, 10882−10888. (c) Camm, K. D.; El-Sokkary, A.; Gott, A. L.; Stockley, P. G.; Belyaeva, T.; McGowan, P. C. *Dalton Trans.* **2009**, 10914−10925.

(3) (a) Meggers, E. *Chem. Commun.* **2009**, 1001−1010. (b) Meggers, E.; Atilla-Gokcumen, G. E.; Bregman, H.; Maksimoska, J.; Mulcahy, S. P.; Pagano, N.; Williams, D. S. *Synlett* **2007**, 1177−1189.

(4) (a) Vives, G.; Jacquot de Rouville, H.-P.; Carella, A.; Launay, J.-P.; Rapenne, G. *Chem. Soc. Rev.* **2009**, *38*, 1551−1561. (b) Vives, G.; Carella, A.; Launay, J.-P.; Rapenne, G. *Coord. Chem. Rev.* **2008**, *252*, 1451−1459. (c) Jacquot de Rouville, H.-P.; Vives, G.; Rapenne, G. *Pure Appl. Chem.* **2008**, *80*, 659−667. (d) Carella, A.; Coudret, C.; Guirado, G.; Rapenne, G.; Vives, G.; Launay, J.-P. *Dalton Trans.* **2007**, 177−186.

(5) (a) Severin, K.; Bergs, R.; Beck, W. *Angew. Chem., Int. Ed.* **1998**, *37*, 1634−1654. (b) Hoffmüller, W.; Maurus, M.; Severin, K.; Beck, W. *Eur. J. Inorg. Chem.* **1998**, 729−731. (c) Krämer, R. *Angew. Chem., Int. Ed.* **1996**, *35*, 1197−1199. (d) Krämer, R.; Maurus, M.; Polborn, K.; Sünkel, K.; Robl, C.; Beck, W. *Chem.—Eur. J.* **1996**, *2*, 1518−1526.

(6) Nagashima, H.; Kondo, H.; Hayashida, T.; Yamaguchi, Y.; Gondo, M.; Masuda, S.; Miyazaki, K.; Matsubara, K.; Kirchner, K. *Coord. Chem. Rev.* **2003**, *245*, 177−190.

(7) (a) Gridnev, I. D.; Watanabe, M.; Wang, H.; Ikariya, T. *J. Am. Chem. Soc.* **2010**, *132*, 16637−16650. (b) Koike, T.; Ikariya, T. *Adv. Synth. Catal.* **2004**, *346*, 37−41.

(8) (a) Koike, T.; Ikariya, T. *J. Organomet. Chem.* **2007**, *692*, 408−419. (b) Pelagatti, P.; Bacchi, A.; Calbiani, F.; Carcelli, M.; Elviri, L.; Pelizzi, C.; Rogolino, D. *J. Organomet. Chem.* **2005**, *690*, 4602−4610.

(9) (a) Albertin, G.; Antoniutti, S.; Castro, J.; Paganelli, S. *J. Organomet. Chem.* **2010**, *695*, 2142−2152. (b) Barboza da Silva, C. F.; Schwarz, S.; Mestres, M. G.; López, S. T.; Strähle, J. *Z. Anorg. Allg. Chem.* **2004**, *630*, 1919−1923.

(10) Brunner, H.; Henning, F.; Zabel, M. *Z. Anorg. Allg. Chem.* **2004**, *630*, 91−96.

(11) Marchetti, F.; Pettinari, C.; Pettinari, R.; Cerquetella, A.; Cingolani, A.; Chan, E. J.; Kozawa, K.; Skelton, B. W.; White, A. H.; Wanke, R.; Kuznetsov, M. L.; Martins, L. M. D. R. S.; Pombeiro, A. J. L. *Inorg. Chem.* **2007**, *46*, 8245−8257.

(12) (a) Kuwata, S.; Ikariya, T. *Dalton Trans.* **2010**, *39*, 2984−2992. (b) Kimura, T.; Arita, H.; Ishiwata, K.; Kuwata, S.; Ikariya, T. *Dalton Trans.* **2009**, 2912−2914. (c) Burell, A. K.; Steedman, A. J. *Organometallics* **1997**, *16*, 1203−1208.

(13) Pelagatti, P.; Carcelli, M.; Calbiani, F.; Cassi, C.; Elviri, L.; Pelizzi, C.; Rizzotti, U.; Rogolino, D. *Organometallics* **2005**, *24*, 5836−5844.

(14) Koike, T.; Ikariya, T. *Organometallics* **2005**, *24*, 724−730.

(15) (a) Pettinari, C.; Marchetti, F.; Cerquetella, A.; Pettinari, R.; Monari, M.; Mac Leod, T. C. O.; Martins, L. M. D. R. S.; Pombeiro, A. J. L. *Organometallics* **2011**, *30*, 1616−1626. (b) Bhambri, S.; Bishop, A.; Kaltsoyannis, N.; Tocher, D. A. *J. Chem. Soc., Dalton Trans.* **1998**, 3379−3390. (c) Bhambri, S.; Tocher, D. A. *J. Chem. Soc., Dalton Trans.* **1997**, 3367−3372. (d) Bhambri, S.; Tocher, D. A. *Polyhedron* **1996**, *15*, 2763−2770. (e) Restivo, R. J.; Ferguson, G.; O'Sullivan, D. J.; Lalor, F. J. *Inorg. Chem.* **1975**, *14*, 3046−3052. (f) Restivo, R. J.; Ferguson, G. *J. Chem. Soc., Chem. Commun.* **1973**, 847−848.

(16) (a) Ciancaleoni, G.; Zuccaccia, C.; Zuccaccia, D.; Clot, E.; Macchioni, A. *Organometallics* **2009**, *28*, 960−967. (b) Zuccaccia, D.; Clot, E.; Macchioni, A. *New. J. Chem.* **2005**, *29*, 430−433.

(17) Bailey, P. J.; Pace, S. *Coord. Chem. Rev.* **2001**, *214*, 91−141.

(18) (a) Bazinet, P.; Wood, D.; Yap, G. P. A; Richeson, D. S. *Inorg. Chem.* **2003**, *42*, 6225−6229. (b) Foley, S. R.; Yap, G. P. A; Richeson, D. S. *Inorg. Chem.* **2002**, *41*, 4149−4157. (c) Foley, S. R.; Yap, G. P. A; Richeson, D. S. *Polyhedron* **2002**, *21*, 619−627. (d) Thirupathi, N.; Yap, G. P. A; Richeson, D. S. *Organometallics* **2000**, *19*, 2573−2579. (e) Foley, S. R.; Yap, G. P. A; Richeson, D. S. *Chem. Commun.* **2000**, 1515−1516. (f) Thirupathi, N.; Yap, G. P. A; Richeson, D. S. *Chem. Commun.* **1999**, 2483−2484. (g) Tin, M. K. T.; Thirupathi, N.; Yap, G. P. A; Richeson, D. S. *J. Chem. Soc., Dalton Trans.* **1999**, 2947−2951. (h) Tin, M. K. T.; Yap, G. P. A; Richeson, D. S. *Inorg. Chem.* **1998**, *37*, 6728−6730.

(19) Edelmann, F. T. In *Advances in Organometallic Chemistry*; Hill, A. F., Fink, M. J., Eds.; Academic Press: New York, 2008; Vol. *57*, Chapter 3, pp 183−352.

(20) (a) Pap, J. S.; Snyder, J. L.; Piccoli, P. M. B.; Berry, J. F. *Inorg. Chem.* **2009**, *48*, 9846−9852. (b) Robinson, S. D.; Sahajpal, A.; Steed, J. *Inorg. Chim. Acta* **2000**, *303*, 265−270. (c) Bailey, P. J.; Grant, K. J.; Mitchell, L. A.; Pace, S.; Parkin, A.; Parsons, S. *J. Chem. Soc., Dalton Trans.* **2000**, 1887−1891. (d) Holman, K. T.; Robinson, S. D.; Sahajpal, A.; Steed, J. W. *J. Chem. Soc., Dalton Trans.* **1999**, 15−18.

(21) Dinger, M. B.; Henderson, W.; Nicholson, B. K. *J. Organomet. Chem.* **1998**, *556*, 75−88.

(22) Bailey, P. J.; Mitchell, L. A.; Parsons, S. *J. Chem. Soc., Dalton Trans.* **1996**, 2839−2841.

(23) Parsons, S.; Elliott, M.; Bailey, P.; Wood, P. Private Communication, 2004, (Identifier: YAGROO) as cited in Cambridge Structural Data Base, version 5.30, November 2008.

(24) Gopi, K.; Rathi, B.; Thirupathi, N. *J. Chem. Sci.* **2010**, *122*, 157−167.

(25) Gopi, K.; Thirupathi, N.; Nethaji, M. *Organometallics* **2011**, *30*, 572−583.

(26) Bennett, M. A.; Huang, T.-N.; Matheson, T. W.; Smith, A. K.; Ittel, S.; Nickerson, W. *Inorg. Synth.* **1982**, *21*, 74−78.

(27) *ENHANCE, Oxford Xcalibur Single Crystal Diffractometer*, version 1.171.34.40; Oxford Diffraction Ltd: Oxford, U.K., 2006.

(28) *CrysAlisPro*, version 1.171.34.40; Oxford Diffraction Ltd: Oxford, U.K., 2006.

(29) *SMART, Bruker Molecular Analysis Research Tool*, version 5.0; Bruker Analytical X-ray Systems: Madison, WI, 2000.

(30) *SAINT-NT*, version 6.04; Bruker Analytical X-ray Systems: Madison, WI, 2001.
(31) Altomare, A.; Cascarano, G.; Giacovazzo, C.; Guagliardi, A.; Burla, M. C.; Polidori, G.; Camalli, M. *J. Appl. Crystallogr.* **1994**, *27*, 435−436.
(32) Sheldrick, G. M. *SHELXL-97, Program for crystal structure refinement*; University of Göttingen: Göttingen, Germany, 1997.
(33) Sheldrick, G. M. *Acta Crystallogr.* **2008**, *A64*, 112−122.
(34) Farrugia, L. J. *J. Appl. Crystallogr.* **1999**, *32*, 837−838.
(35) Brandenburg, K. *DIAMOND*, version 2.0 c; University of Bonn: Bonn, Germany, 2004.
(36) Singh, K. S.; Svitlyk, V.; Mozharivskyj, Y. *Dalton Trans.* **2011**, *40*, 1020−1023.
(37) Chen, C.-K.; Tong, H.-C.; Hsu, C-Y. C.; Lee, C.-Y.; Fong, Y. H.; Chuang, Y.-S.; Lo, Y.-H.; Lin, Y.-C.; Wang, Y. *Organometallics* **2009**, *28*, 3358−3368.
(38) Nongbri, S. L.; Das, B.; Mohan Rao, K. *J. Organomet. Chem.* **2009**, *694*, 3881−3891.
(39) Lalrempuia, R.; Yennawar, H. P.; Kollipara, M. R. *J. Coord. Chem.* **2009**, *62*, 3661−3678.
(40) Pachhunga, K.; Therrien, B.; Kollipara, M. R. *Inorg. Chim. Acta* **2008**, *361*, 3294−3300.
(41) Ng, S. Y.; Fang, G.; Leong, W. K.; Goh, L. Y.; Garland, M. V. *Eur. J. Inorg. Chem.* **2007**, 452−462.
(42) Singh, K. S.; Kreisel, K. A.; Yap, G. P. A; Kollipara, M. R. *J. Organomet. Chem.* **2006**, *691*, 3509−3518.
(43) Singh, K. S.; Thöne, C.; Kollipara, M. R. *J. Organomet. Chem.* **2005**, *690*, 4222−4231.
(44) Chang, C.-W.; Lee, G.-H. *Organometallics* **2003**, *22*, 3107−3116.
(45) Frühauf, H.-W. *Chem. Rev.* **1997**, *97*, 523−596.
(46) Dori, Z.; Ziolo, R. F. *Chem. Rev.* **1973**, *73*, 247−254.
(47) Häfelinger, G.; Kuske, F. K. H. In *The Chemistry of Amidines and Imidates*; Patai, S., Rappoport, Z., Eds.; Wiley: Chichester, U.K., 1991; Vol. 2.
(48) (a) Kenney, A. P.; Yap, G. P. A; Richeson, D. S.; Barry, S. T. *Inorg. Chem.* **2005**, *44*, 2926−2933. (b) Aeilts, S. L.; Coles, M. P.; Swenson, D. C.; Jordan, R. F.; Young, V. G. Jr. *Organometallics* **1998**, *17*, 3265−3270.
(49) *Syn-syn*, *syn-anti*, *anti-syn*, and *anti-anti* nomenclature used in the present publication for guanidinate ligands differs from that used in reference 24 wherein the nomenclature was based on the orientation of the aryl moiety of the NHAr unit with respect to the C═N bond. Further, α and β indicate upward and downward orientation of the *o*-substituent of the aryl rings with respect to the CN_3 plane of the guanidine.
(50) Zhang, J.; Cai, R.; Weng, L.; Zhou, X. *Organometallics* **2004**, *23*, 3303−3308.
(51) Yadav, M.; Singh, A. K.; Maiti, B.; Pandey, D. S. *Inorg. Chem.* **2009**, *48*, 7593−7603.
(52) Schmid, W. F.; John, R. O.; Mühlgassner, G.; Heffeter, P.; Jakupec, M. A.; Galanski, M.; Berger, W.; Arion, V. B.; Keppler, B. K. *J. Med. Chem.* **2007**, *50*, 6343−6355.
(53) (a) Zuccaccia, D.; Bellachioma, G.; Cardaci, G.; Ciancaleoni, G.; Zuccaccia, C.; Clot, E.; Macchioni, A. *Organometallics* **2007**, *26*, 3930−3946. (b) Schmid, W. F.; John, R. O.; Arion, V. B.; Jakupec, M. A.; Keppler, B. K. *Organometallics* **2007**, *26*, 6643−6652.
(54) Ciancaleoni, G.; Bellachioma, G.; Cardaci, G.; Ricci, G.; Ruzziconi, R.; Zuccaccia, D.; Macchioni, A. *J. Organomet. Chem.* **2006**, *691*, 165−173.
(55) Zuccaccia, D.; Macchioni, A. *Organometallics* **2005**, *24*, 3476−3486.
(56) Chen, H.; Parkinson, J. A.; Parsons, S.; Coxall, R. A.; Gould, R. O.; Sadler, P. J. *J. Am. Chem. Soc.* **2002**, *124*, 3064−3082.
(57) Carmona, D.; Ferrer, J.; Oro, L. A.; Apreda, M. C.; Foces-Foces, C.; Cano, F. H.; Elguero, J.; Jimeno, M. L. *J. Chem. Soc., Dalton Trans.* **1990**, 1463−1476.
(58) Gossens, C.; Tavernelli, I.; Rothlisberger, U. *J. Chem. Theory Comput.* **2007**, *3*, 1212−1222.
(59) Peacock, A. F. A.; Melchart, M.; Deeth, R. J.; Habtemariam, A.; Parsons, S.; Sadler, P. J. *Chem.—Eur. J.* **2007**, *13*, 2601−2613.
(60) Lang, R.; Polborn, K.; Severin, T.; Severin, K. *Inorg. Chim. Acta* **1999**, *294*, 62−67.
(61) (a) Lampeka, R.; Bergs, R.; Fernández de Bobadilla, R.; Polborn, K.; Mihan, S.; Beck, W. *J. Organomet. Chem.* **1995**, *491*, 203−214. (b) Krämer, R.; Maurus, M.; Bergs, R.; Polborn, K.; Sünkel, K.; Wagner, B.; Beck, W. *Chem. Ber.* **1993**, *126*, 1969−1980.
(62) Mullins, S. M.; Duncan, A. P.; Bergman, R. G.; Arnold, J. *Inorg. Chem.* **2001**, *40*, 6952−6963.
(63) Milanov, A.; Bhakta, R.; Baunemann, A.; Becker, H.-W.; Thomas, R.; Ehrhart, P.; Winter, M.; Devi, A. *Inorg. Chem.* **2006**, *45*, 11008−11018.
(64) Howell, J. A. S.; Burkinshaw, P. M. *Chem. Rev.* **1983**, *83*, 557−599.
(65) Ramanathan, S.; Lemal, D. M. *J. Org. Chem.* **2007**, *72*, 1566−1569.
(66) (a) Li, X.; Curran, D. P. *Org. Lett.* **2010**, *12*, 612−614. (b) Ototake, N.; Nakamura, M.; Dobashi, Y.; Fukaya, H.; Kitagawa, O. *Chem.—Eur. J.* **2009**, *15*, 5090−5095, , and references cited therein.
(67) Liu, F.-C.; Lin, Y. L.; Yang, P.-S.; Lee, G.-H.; Peng, S.-M. *Organometallics* **2010**, *29*, 4282−4290, , and references cited therein.
(68) Romeo, R.; Carnabuci, S.; Fenech, L.; Plutino, M. R.; Albinati, A. *Angew. Chem., Int. Ed.* **2006**, *45*, 4494−4498.
(69) Faller, J. W.; Parr, J.; Lavoie, A. R. *New. J. Chem.* **2003**, *27*, 899−901.